Investigation Into Nanofluid Based Double Tube Heat Exchanger

A Dissertation submitted
in partial fulfilment of the requirements
for the award of degree of

Master of Engineering

in

Thermal Engineering

by

Darshan M B

Registration No.: 801483008

Under the Supervision of

Mr. Kundan Lal

(Assistant Professor)

(MED, Thapar University)

DEPARTMENT OF MECHANICAL ENGINEERING

THAPAR UNIVERSITY, PATIALA

July, 2016

CERTIFICATE

I hereby declare that the thesis entitled "**Investigation into nanofluid based double tube heat exchanger**" is an authentic record of my work carried out as requirements for the award of the degree of **Master of Engineering** in Thermal Engineering at **Thapar University, Patiala, Punjab** under the supervision of **Mr. Kundan Lal**, Assistant Professor, Mechanical Department, Thapar University, Patiala during July, 2014 to July, 2016. No part of the matter embodied in this report has been submitted to any other university or institute for the award of any degree.

Date: 8/07/2016

Darshan M B

It is certified that the above statement made by the student is correct to the best of my/our knowledge and belief.

Mr. Kundan Lal
Assistant Professor
Mechanical Engineering Department
Thapar University, Patiala – 147004

Countersigned by

Head, Mechanical Engineering Department
Thapar University, Patiala – 147004

Dean of Academic Affairs
Thapar University, Patiala - 147004

ii

Dedication

I dedicate this thesis to my beloved father Basavaraja D N and my mother Dakshayinidevi B S, who have supported me throughout. I also dedicate this to my brother Indudhara B, who is as an impression for me and to all my dearest friends.

Acknowledgements

First of all, I would like to thank my most esteemed supervisor Mr. Kundan lal, Assistant Professor, Thapar University, Patiala for his worthy guidance, continuous encouragement and having high patience to listen to all my queries and suggest accordingly. The freedom Mr. Kundan Lal Sir gave me for doing my thesis and his faith in me always compelled me to work hard.

I would like to acknowledge all the members of mechanical labs and chemical labs, Thapar University for helping me out in solving any problems that occured while carrying out experimental work.

I appreciate the facilities provided by Thapar University to carry out my studies and gain practical knowledge.

A special debt of gratitude is owed to the authors whose work I have consulted and quoted in this work.

Last but not least I am always grateful to my family and friends for their unconditional support, encouragement and best wishes.

Abstract

Investigations into heat transfer characteristics of the internal flows have been of prime importance for many engineering applications. This thesis reports an experimental and numerical study on the forced convective heat transfer and flow characteristics of a TiO_2-H_2O nanofluid (0.05 % and 0.026 % volume concentration). The heat transfer coefficient and friction factor of the TiO_2-H_2O nanofluid flowing in a horizontal double-tube counter flow heat exchanger, with and without twisted tape inserts under turbulent flow conditions have been investigated experimentally. The twisted tapes of twist ratio 3.2, 4 and 6 have been considered for this purpose. Furthermore, a numerical study has been conducted with different nanoparticles (TiO_2, Al_2O_3 and CuO) with their varying concentration and size under turbulent flow conditions. Numerical investigation is done in ANSYS Fluent 14.5 software. The experimental and numerical investigations have been conducted in Reynolds number range of 5000 to 25000. Experimental results show that the convective heat transfer coefficient of TiO_2-H_2O nanofluid of 0.05% volumetric concentration is slightly higher than that of the base fluid by 4-6 %. Also, with 0.05% TiO_2-H_2O nanofluid in a tube with twisted tape of twist ratio 3.2, the heat transfer coefficient is found to increase by 1.45 times the value of the heat transfer coefficient when water is used as a working fluid in a plain tube. Numerically, a comparison is made between single phase and two phase Computational Fluid Dynamics (CFD) models. For the problem under consideration the two phase model (mixture model) gives closer predictions of the convective heat transfer coefficient to the experimental data than the single-phase model. Numerical investigations show that, for 1% volumetric concentration, among the three nanoparticle considered, Al_2O_3 gives higher enhancement of heat transfer coefficient. Also, at lower volumetric concentrations of nanoparticle, varying the particle size does not cause significant difference in heat transfer coefficient .

Keywords: Nanofluid; CFD; Multiphase flow; Heat exchanger, turbulators.

TABLE OF CONTENTS

LIST OF FIGURES

LIST OF TABLES

LIST OF SYMBOLS AND ABBREVIATIONS

Nomenclature

A_o	:	Cross section area of outer tube (m^2)
A_i	:	Cross section area of inner tube (m^2)
C_{pbf}	:	Specific heat of base fluid (J/kgK)
C_{pnf}	:	Specific heat of nanofluid (J/kgK)
C_{pp}	:	Specific heat of nanoparticle (J/kgK)
D	:	Diameter of the tube
f	:	Friction factor
f_p	:	Friction factor for plain tube
f_t	:	Friction factor for tube with twisted tape
f_v	:	Volumetric concentration
F_d	:	Drag force (N)
F_{lift}	:	Lift force (N)
h	:	Heat transfer coefficient (W/m^2K)
h_p	:	Heat transfer coefficient of plain tube (W/m^2K)
h_t	:	Heat transfer coefficient of tube with twisted tape (W/m^2K)
k_{nf}	:	Thermal conductivity of nanofluid (W/mK)
k_p	:	Thermal conductivity of nanoparticle (W/mK)
k_w	:	Thermal conductivity of water (W/mK)
Nu	:	Nusselt number
Pr	:	Prandtle number
∇P	:	Pressure drop (kPa)
Q	:	Heat transfer rate (W)
Re	:	Reynolds number
T	:	Temperature
U	:	Velocity of the fluid (m/s)
v_{np}	:	Volume of nanoparticle (m^3)
v_{bf}	:	Volume of base fluid (m^3)

V_m : Velocity of mixture (m/s)

y_o : Pitch of twisted tape (cm)

W : Width of twisted tape (cm)

Greek symbols

η : Thermal performance factor

μ_{bf} : Viscosity of base fluid (Ns/m^2)

μ_{nf} : Viscosity of nanofluid (Ns/m^2)

ρ_{bf} : Density of base fluid (kg/m^3)

ρ_{nf} : Density of nanofluid (kg/m^3)

ρ_p : Density of nanoparticle (kg/m^3)

τ_w : Wall shear stress (Pa)

$\boldsymbol{\phi}$: Volumetric concentration of nanoparticles.

Acronym

CFD : Computational Fluid Dynamics

PID : Proportion Integral Derivative controller

VOF : Volume of Fluid

Chapter 1

Introduction

1.1 Introduction to Heat Exchangers

A heat exchanger is equipment built for efficient heat transfer from one medium to another. The media may be separated by a solid wall to prevent mixing or they may be in direct contact.

They are widely used in space heating, refrigeration, air conditioning, power plants, chemical plants, petrochemical plants, petroleum refineries, natural gas processing, and sewage treatment. Some of the common applications of heat exchangers are as follows:

1. Oil cooling (oil of the engine main lubrication circuit, the manual and automatic transmission, the power steering etc.).
2. Condensers and evaporators for air-conditioning systems (Also called special heat exchangers as the fluids remain in the specific phase only loose sensible heat).
3. Charge air, exhaust gas and fuel cooling.

1.2 Need for Enhancement of Heat Transfer in Heat Exchangers

Heat exchangers play a vital role in several engineering applications, such as automobile, aerospace, chemical processing, electronic chip cooling, heat pumps, and energy systems. The thermal performance of heat exchangers depends on a variety of factors including geometric, kinetic and spatial aspects, related to the net heat transfer rate encountered between the heat transfer sections and flow of fluids. More often, the fluids subjected to flow in heat exchangers (either parallel or counter or crossed flow methods) would experience transient thermal conditions throughout the heat transfer processes.

The issues that are commonly faced in heat exchangers are in terms of incongruent heat exchange mechanism between the heat sources (or sink) and the fluid medium, reduced effectiveness on long term use, decreased heat transport due to scaling, frictional pressure drop, pumping power consumption, and so on. The extensive research for developing value-added engineering systems, which would effectively bridge the gap between transferring the

available process heat relative to the rheological behaviour of flowing fluids, is of increasing concern worldwide.

The heat exchange phenomenon between the fluid and surrounding high temperature source is governed by convective heat transfer. In the current era, high performance heat transfer equipment with minimal surface area is the industrial requirement. Also, to derive optimal energy conversion, the design of the system must provide high efficiency at low cost. The enhancement of heat dissipation to the working fluid and using a working fluid of high heat transfer performance will increase the efficiency of heat exchangers. Some of the reasons for requirement of high heat transfer performance can be as follows:

1. The heat rejection requirements are continually increasing due to trends toward faster speeds (in the multi-GHz range) and smaller features (to <100 nm) for microelectronic devices, more power output for engines.

2. Cooling becomes one of the top technical challenges facing high-tech industries such as microelectronics, transportation, and manufacturing.
3. Current cooling techniques not adequate:For instance, future processors for high performance computers may require removal rates of 1000W/cm^2: air cooling realistic below 100W/cm^2.

The enhancement of heating or cooling in an industrial process may create

1. A saving in energy.

2. Reduce process time.

3. raise thermal rating and

4. Lengthen the working life of equipment.

Conversely a new approach to enhancing heat transfer to encounter the cooling challenge is necessary because of the increasing need for more efficient heat transfer fluids in many industries, such as the electronics industries, photonics industries, transportation industries, and energy supply industries. The conventional way to enhance the heat transfer rate in thermal systems is to increase the heat transfer by increasing surface area of cooling devices and the flow velocity or to disperse solid particles in heat transfer fluids.

In the development of energy-efficient heat transfer fluids, the thermal conductivity of the heat transfer fluids plays a vital role. Despite considerable previous research and

development efforts on heat transfer enhancement, major improvements in cooling capabilities have been constrained because traditional heat transfer fluids used in today's thermal management systems, such as water, oils, and ethylene glycol, have inherently poor thermal conductivities, orders-of-magnitude smaller than those of most solids. Due to increasing global competition, a number of industries have a strong need to develop advanced heat transfer fluids with significantly higher thermal conductivities than are presently available. Therefore fluids with suspended particles are expected to have better heat transfer properties.

1.3 Addition of Micron Sized Particles and its Disadvantages

High thermal conductivity of solids can be used to increase the thermal conductivity of a fluid by adding small solid particles to that fluid. The feasibility of the usage of such suspensions of solid particles with sizes on the order of 2 millimetres or micrometres was previously investigated by several researchers and the following significant drawbacks were observed,

1. The particles settle rapidly, forming a layer on the surface and reducing the heat transfer capacity of the fluid.
2. If the circulation rate of the fluid is increased, sedimentation is reduced, but the erosion of the heat transfer devices, pipelines, etc., increases rapidly.
3. The large size of the particles tends to clog the flow channels, particularly if the cooling channels are narrow.
4. The pressure drop in the fluid increases considerably.
5. Finally, conductivity enhancement based on particle concentration is achieved (i.e., the greater the particle volume fraction is, the greater the enhancement—and greater the problems, as indicated above). To be efficient, these conventional fluid suspensions uses over 10 vol. % of solid particles, resulting in significantly greater pressure drop and pump power.

Therefore, before the introduction of nanofluids, the route of suspending particles in liquid was a well-known but rejected option for heat transfer applications.

1.4 Nanofluids

The emergence of modern materials technology provided the opportunity to produce nanometre-sized particles which are quite different from the parent material in mechanical, thermal, electrical, and optical properties. Various research efforts taken by scientists and engineers in tuning the material properties at the nanoscale level; have indubitably led to finding solutions for the aforementioned challenges, in improving the thermal performance of heat exchangers. The incorporation of specialized fluids that are engineered towards improving the thermal performance of heat exchangers has become increasingly attractive in recent years.

Nanofluids which are a mixture of nano-sized (1nm-100 nm) particles (nanoparticles) suspended in a base fluid, are used to enhance the heat transfer rate, via its improved thermophysical properties compared to the base fluid. Since solid materials possess higher thermal conductivities than base fluid. Nanofluids have been projected as a next generation fluid capable of superior heat transfer when compared to conventional heat transfer fluids for a given set of conditions. With very small volume fraction of such nanoparticles the thermal conductivity and convective heat transfer capability of these suspensions are significantly enhanced without the problems encountered in various types of slurries such as high pumping power, clogging, erosion, sedimentation. Nanoparticles stay suspended much longer and possess a much higher surface area. The surface to volume ratio of nanoparticles is 1000 times larger than that of microparticles. The high surface area of nanoparticles improves the heat conduction of nanofluids since heat transfer occurs on the surface of the particle.

Modern nanotechnology can produce various types of metallic or non-metallic particles of nanometer sizes. Nanoparticle materials have exclusive chemical properties, mechanical properties, optical, electrical properties, magnetic properties, & thermal properties. Nano fluids (nanoparticle fluid suspensions) is the term invented by Choi et al. (1995) to describes this new generation of nanotechnology-based heat transfer fluids that exhibited thermal properties higher to those of their host fluids or conventional particle fluid suspensions. Nano fluid technology, a new inter disciplinary field of great importance where nano sciences, nanotechnology, and thermal engineering encounter, has developed largely over the past decade. The goal of nanofluids is to achieve the highest possible thermal properties at the smallest possible concentrations (preferably < 1% by volume).

1.5 Materials for Nanoparticles and Base Liquid Used

Nanoparticle materials include:

1. Oxide ceramics – Al_2O_3, CuO
2. Metal carbides – SiC
3. Nitrides – AlN, SiN
4. Metals – Al, Cu
5. Non-metals – Graphite, carbon nanotubes

Base fluids include:

1. Water
2. Ethylene- or tri-ethylene-glycols and other coolants
3. Oil and other lubricants

1.6 Preparation Methods for Nanofluids

The optimization of nanofluid's thermophysical properties requires successful synthesis procedures for creating stable suspensions of nanoparticles in liquids. Depending on the requirements of a particular application, many combinations of particle materials and fluids are of potential interest. For example, nanoparticles of oxides, carbides, metals and non-metals can be dispersed into the conventional fluids such as deionized (DI) water, ethylene glycol (EG), or engine oil. In the following description, two major methods generally used for the production of nanofluids are explained below.

1.6.1 Two-Step Method

Two-step method is the most widely used method for preparing nanofluids. Nanoparticles, nanofibers, nanotubes, or other nanomaterials used in this method are first produced as dry powders by chemical or physical methods. Then, the nanosized powder will be dispersed into a fluid in the second processing step with the help of intensive magnetic force agitation, ultrasonic agitation, high-shear mixing, homogenizing, and ball milling. Two-step method is the most economic method to produce nanofluids in large scale, because nanopowder synthesis techniques have already been scaled up to industrial production levels. Due to the high surface area and surface activity, nanoparticles have the tendency to aggregate. The important technique to enhance the stability of nanoparticles in fluids is the use of

surfactants. However, the functionality of the surfactants under high temperature is also a big concern, especially for high-temperature applications.

Due to the difficulty in preparing stable nanofluids by two-step method, several advanced techniques are developed to produce nanofluids, including one-step method.

1.6.2 One-Step Method

To reduce the agglomeration of nanoparticles, Eastman et al. developed a one-step physical vapour condensation method to prepare Cu/ethylene glycol nanofluids. The one-step process consists of simultaneously making and dispersing the particles in the fluid. In this method, the processes of drying, storage, transportation, and dispersion of nanoparticles are avoided, so the agglomeration of nanoparticles is minimized, and the stability of fluids is increased. The one-step processes can prepare uniformly dispersed nanoparticles, and the particles can be stably suspended in the base fluid.

One-step physical method cannot synthesize nanofluids in large scale, and the cost is also high, so the one-step chemical method is developing rapidly. However, there are some disadvantages for one-step method. The most important one is that the residual reactants are left in the nanofluids due to incomplete reaction or stabilization. It is difficult to elucidate the nanoparticle effect without eliminating this impurity effect.

1.7 Computational Fluid Dynamics and Nanofluids

Computational Fluid Dynamics (CFD) is a way of predicting results of a fluid flow by solving the mathematical models governing the fluid flow. Most of the time, the fluid flow is also associated with heat transfer, mass transfer, chemical reaction, phase change etc. CFD is an interdisciplinary branch (Figure 1.1) which requires the knowledge of mathematical modelling or numerical analysis, computer science and fluid mechanics to solve a fluid flow problem. CFD process involves; converting the governing differential or integral equation into a set of algebraic equations and then solving these algebraic equation using high speed computers.

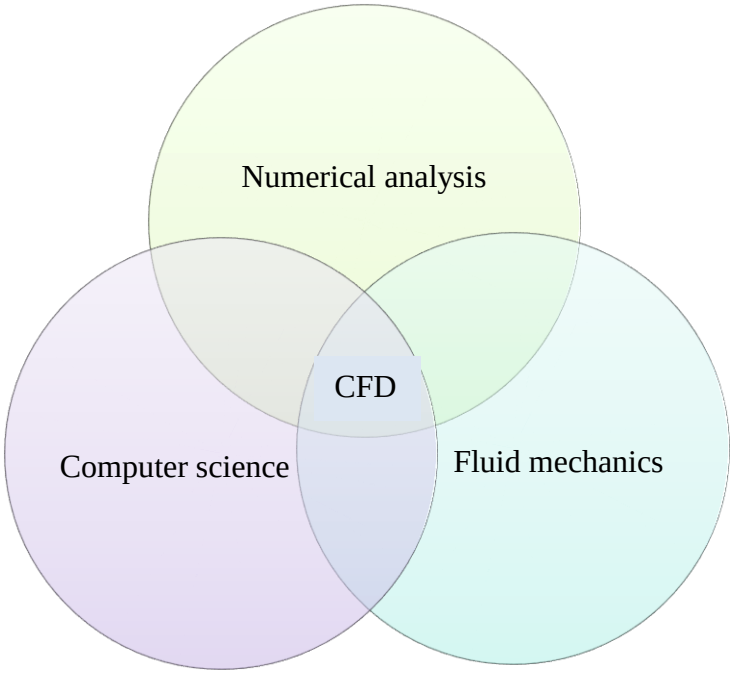

Figure 1.1: CFD as an interdisciplinary branch

Some of the applications of CFD are as follows,

1. Aerodynamics of vehicles.
2. Power plants
3. Weather predictions
4. Hydrology and oceanography
5. Environmental engineering
6. Biomedical engineering applications.
7. Combustion in IC engines
8. Sports

1.7.1 Methodology

Any problem solved using computational fluid dynamic technique includes three main steps, namely

1. Pre-processing
2. Solving
3. Post-processing

Figure 1.2 shows a simple flowchart of steps followed in CFD.

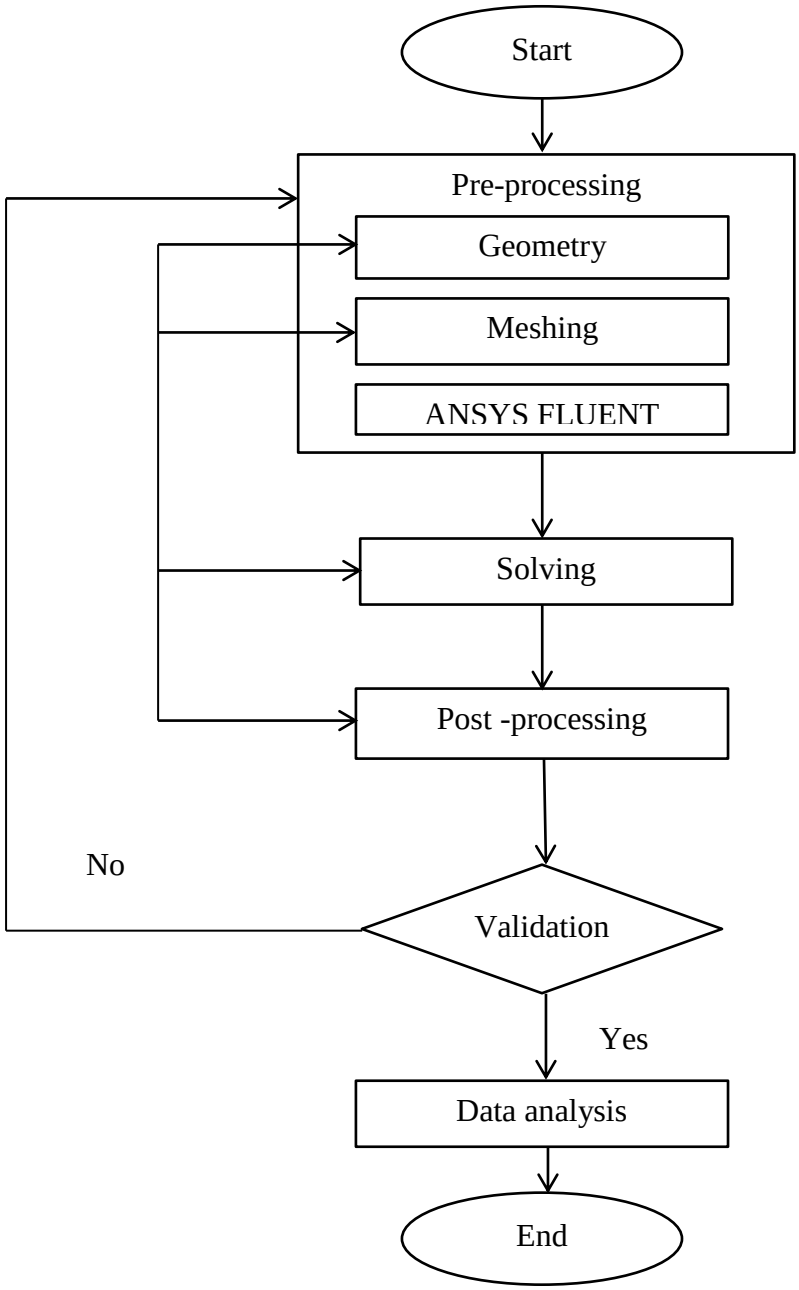

Figure 1.2: Flowchart of CFD

1. Pre-processing:

Pre-processing is the first step for any CFD problem. Pre-processing is the step where,

- Geometry is defined with dimensions.
- The selected geometry is meshed. Meshing is nothing but dividing the given geometry into number of small elements.
- Define the different surfaces like inlet, outlet, wall etc., as required.
- Setup the boundary conditions.

2. Solving:

Any fluid flow problem can be governed by a set of equations called governing equation. To obtain the solution for the fluid flow problem these governing equations needs to be solved. Solver in the CFD solves these governing equations in two steps.

- A set of algebraic equations are obtained from these governing equations. This process is called discretization.
- Then the algebraic equations are solved iteratively to obtain the solution.

3. Post-processing:

The results of the problem can be seen in post processing. Plots, contours, graphs and numerical values can be seen in post processing. The CFD result includes some errors because of many approximations used while solving the problem. Hence, the results should be validated with any available experimental or standard data. If the results obtained from CFD are comparable to the standard data then the result is said to be validated. If not, changes should be made in post processing to obtain the correct results.

1.7.2 CFD Models

A fluid flow problem like nanofluids which has solid particles dispersed in a fluid medium is essentially a two phase flow. These types of flows can be solved in two ways. They are,

1. Single phase model:

   Nanofluid is made by dispersing solid particles in a fluid. Hence, nanofluid is essentially two phase (solid-liquid). But, in the single phase model nanofluid is assumed to be a single phase fluid. The addition of nanoparticles to the fluid results in changes in some properties of the fluid like density, viscosity, specific heat, thermal conductivity etc. Hence, the properties of the nanofluid are calculated by using available correlations. These values are then input into the system. In general, single phase model solves the differential equations of mass, momentum and energy for fluid with effective properties. The equations used for calculating effective properties of nanofluid are given below.

   Density of the nanofluid is given by,

   $$\rho_{nf} = \phi\rho_p + (1-\phi)\rho_{bf} \quad (1.1)$$

Where, ρ_{nf}, ρ_{bf}, ρ_p denotes density of nanofluid, base fluid and nanoparticle respectively and $\boldsymbol{\phi}$ is the concentration of nanoparticles used.

Viscosity of the nanofluid is given by,

$$\mu_{nf} = (1 + 2.5\phi)\mu_{bf} \quad (1.2)$$

Where, μ_{nf} and μ_{bf} represents viscosity of nanofluid and base fluid respectively

Specific heat of the nanofluid is given by,

$$C_{p_{nf}} = \frac{(1-\phi)\rho_{bf}C_{p_{bf}} + \phi\rho_p C_{p_p}}{\rho_{nf}} \quad (1.3)$$

Where, $C_{p_{nf}}$, $C_{p_{bf}}$ and C_{p_p} are the specific heat of nanofluid, base fluid and nanoparticle respectively.

Thermal conductivity of the nanofluid is given by

$$K_{nf} = \frac{k_p + 2k_w + 2(k_p - k_w)}{k_p + 2k_w - (k_p - k_w)} * k_w \quad (1.4)$$

The governing equations solved in single phase model are as follows,

$$\frac{\partial \rho}{\partial t} + \nabla.(\rho U) = 0 \quad (1.5)$$

$$\frac{\partial (\rho U)}{\partial t} + \nabla.(\rho UU) = -\nabla P + \nabla\tau + \rho g \quad (1.6)$$

$$\frac{\partial (\rho h)}{\partial t} + \nabla.\left(\rho U C_p T\right) = \nabla.(k\nabla T) \quad (1.7)$$

Equations (1.5), (1.6) and (1.7) represent the conservation equations of mass, momentum and energy in differential form, respectively.

2. Multiphase model:

In multiphase model, the nanoparticle and the fluid are treated as separate phases. There are two approaches in multiphase modeling, Eulerian-Eulerian approach and Eulerian-Lagrangian approach. Eulerian-Eulerian approach is the best suited for nanofluids and hence only this approach is discussed here. There are three different types of Eulerian-Eulerian approach and are discussed below.

- Volume of Fraction model (VOF)

  In VOF model, velocity components are found out by solving one momentum equation and are shared by all the phases. The equation for mass conservation is given as,

  $$\nabla.\left(\phi_q \rho_q \overrightarrow{V_q}\right) = 0 \quad (1.8)$$

  Any property, N, is calculated by using the equation given below.

  $$N = \sum_{q=1}^{n} \phi_q N_q \quad (1.9)$$

The momentum and energy conservation equations used in this model are same as Eqs. (1.6) and (1.7), respectively.

- Mixture model

The mixture model solves the following governing equations,

Continuity equation: $\nabla.(\rho_m V_m) = 0$ (1.10)

Where, density of mixture ρ_m is given by

$\rho_m = \boldsymbol{\phi}\rho_p + (1- \boldsymbol{\phi})\,\rho_{bf}$ (1.11)

Where, $\boldsymbol{\phi}$ is the volumetric concentration of nanoparticle in base fluid.

Conservation of momentum equation:

$\nabla.(\rho_m V_m V_m) = -\nabla P + \nabla.(\mu_m.\nabla V_m) + \nabla.\sum_{k=1}^{n}\phi_k\rho_k V_{dr,k}V_{dr,k} + \rho_m g$ (1.12)

Drift velocity $V_{dr,k}$ is calculated by $V_{dr,k} = V_k - V_m$ (1.13)

Conservation of energy equation:

$\nabla.\sum_{k=1}^{n}(\phi_k.\rho_k.C_{p,k}.V_k.T) = \nabla.(k_m.\nabla T)$ (1.14)

Volume fraction equation:

$\nabla.(\phi_p\rho_p V_m) = -\nabla.(\phi_p\rho_p V_{dr,p})$ (1.15)

Where mass average velocity V_m is calculated by

$V_m = \frac{\sum_{k=1}^{n}(\phi_k.\rho_k.V_k)}{\rho_m}$ (1.16)

- Eulerian model

In Eulerian model, the conservation equations of mass, momentum and energy are solved separately for different phases. The governing equations used in Eulerian model are given below.

Conservation of mass,

$\nabla.(\phi_q\rho_q\overrightarrow{V_q}) = 0$ (1.17)

Conservation equation of momentum for q^{th} phase is given by,

$\nabla.(\phi_q\rho_q\overrightarrow{V}\,\overrightarrow{V}) = -\phi_q\nabla P + \phi_q\nabla.(\mu_q.\nabla\overrightarrow{V}) + \phi_q\rho_q\vec{g} + F_d + F_{lift}$ (1.18)

Where, F_d and F_{lift} are drag and lift forces respectively. Lift forces can be neglected for nanofluids since the size of particles is very less. Drag force can be calculated by,

$$F_d = \beta(V_l - V_p) \tag{1.19}$$

Where, β is the friction coefficient and is given by,

$$\beta = \frac{3}{4} C_d \frac{\phi_l(1-\phi_l)}{d_p} \rho_l \left|\overrightarrow{V_l} - \overrightarrow{V_p}\right| \phi_l^{-2.65} \tag{1.20}$$

Drag coefficient C_d is given by,

$$C_d = \begin{cases} \frac{24}{Re_p}(1 + 0.15Re_p{}^{0.687} & Re_p < 1000 \\ 0.44 & Re_p \geq 1000 \end{cases} \tag{1.21}$$

$$\text{Where, } Re_p = \frac{\phi_l \rho_l \left|\overrightarrow{V_l} - \overrightarrow{V_p}\right| d_p}{\mu_l} \tag{1.22}$$

Conservation of energy,

$$\nabla.\left(\phi_q \rho_q \overrightarrow{V_q} H_q\right) = -\nabla.\left(K_q \nabla. T_q\right) - \tau_q : \nabla\overrightarrow{V_q} + \sum_{p=1}^{n} \overrightarrow{Q_{pq}} \tag{1.23}$$

Where, heat exchange coefficient Q_{pq} is given by

$$\overrightarrow{Q_{pq}} = h(\overrightarrow{V_p} - \overrightarrow{V_q}) \tag{1.24}$$

$$h = (6K_q \phi_q \phi_p Nu_p)/d_p^2 \tag{1.25}$$

$$Nu_p = 2 + 0.6Re^{0.5} Pr_q^{0.333} \tag{1.26}$$

$$Pr_q = (C_{p_q} \mu_q)/K_q \tag{1.27}$$

Chapter 2

Literature Review

Heat exchanger, as said in the introduction is a device used for efficient heat transfer from one medium to another. Some of the common places where heat exchangers are used include automobiles, electronic chip cooling, chemical processing industries, aerospace, heat pumps and energy systems. The net heat transfer rate between the heat transfer sections and flowing fluids depends on many factors including geometric, spatial and kinetic aspects which in turn determines the performance of heat exchangers. During the heat transfer process the fluid flowing in the heat exchanger experiences transient thermal conditions.

The common problems that arise in heat exchangers are in terms of inconsistent heat exchange mechanism between the heat sources/sink and the fluid medium, reduction in effectiveness after many cycles, scaling on pipes, which affects heat transfer, pressure drop and power consumed for pumping the heat transfer fluids.

To overcome the problems mentioned above and to improve the performance of heat exchangers, various researches are being done by scientists. One of them includes looking into the material properties at nano-level, which led to finding of specialized fluids called nanofluids. Nanofluids are a class of heat transfer fluids having high thermal conductivity particles of sizes in the range of 1-100 nm, dispersed in the fluid medium. Many researches done before have shown that addition of small amount of these thermally conductive nanoparticles results in enhancement of thermo physical and transport properties of the base fluids. The improvements of thermophysical and transport properties of the base fluids in turn results in improvement of performance of heat exchangers. Because of this extensive research is going on in the field of nanofluids to explain and predict the behaviour of these fluids at different conditions. The following section gives a brief idea of various researches on nanofluids and their effects on heat transfer based on available literatures.

Duangthongsuk et al. (2009) conducted an experimental study of TiO_2-water nanofluid in a horizontal double tube heat exchanger. The double tube heat exchanger was of 1.5 m long with inner tube made of copper having inner and outer diameter of 8.13 mm and 9.53 respectively. The outer tube is made of PVC having inner and outer diameter of 27.8 mm and 33.9 mm. Reynolds number range used is 4000- 19000. Experiments were conducted

for different nanofluid temperature (15 ^{0}C, 20 ^{0}C and 25 ^{0}C) to see the effect of temperature on heat transfer rate. For 0.2% concentration the improvement in heat transfer coefficient was observed to be nearly 6 to 11%. They also observed that the heat transfer rate is more when nanofluid temperature is less. Also, since the concentration is very less, they found that the pressure drop and friction factor for the nanofluid is same as that of water.

Namburu et al. (2009) numerically studied the heat transfer characteristics of CuO, SiO_2 and Al_2O_3 dispersed in a base fluid which is a mixture of ethylene glycol and water flowing in turbulent flow regime. They also carried out simulations for various diameters of nanoparticle to check the effect of size of nanoparticle on Nusselt number. The nanofluid was considered to be a single phase fluid with enhanced properties like thermal conductivity, viscosity, density compared to the pure ethylene glycol-water mixture. The geometry selected for the study is a 2-dimensional circular tube with 0.01 m diameter and 0.8 m length. The boundary conditions used were, uniform velocity, outflow and constant heat flux (50 W/m^2) at inlet, outlet and wall respectively. Coupling of pressure and velocity was done using SIMPLE method. The geometry was divided into a grid of 100 x 150. They observed that at 6% concentration and at lower Reynolds number (Re=20000) there is an increase in Nusselt number by 1.35 times compared to that of base fluid, while it is 1.23 times at higher Reynolds number (Re=100000) . Therefore, they concluded that the effect of adding nanoparticles is more significant at low Reynolds number. Among the different nanofluids, CuO- EG/water nanofluid shows highest increase in heat transfer coefficient.

Vajja et al. (2010) in their research paper gave common correlations for heat transfer coefficient and friction factor of nanofluids prepared by dispersing Copper oxide, aluminium oxide and silicon dioxide in water-ethylene glycol mixture base fluid. The experimental setup used by them included a copper tube with nominal diameter of 4.76 mm. Electric resistance strip heaters ensure constant heat flux boundary condition. They used nanofluids having particle concentrations of 1%, 2%, 4%, 6 %, 8%, and 10%. The base fluid used was EG/W mixture in the ratio 60:40. They found that at Reynolds number of 10000, considering nanofluids of 6% concentration of SiO_2, Al_2O_3 and CuO nanoparticles, CuO had maximum increase in heat transfer coefficient of nearly 43% compared to the base fluid. Remaining two i.e. SiO_2 and Al_2O_3 had an increase of 29% and 40% respectively. The new Nusselt number correlation they suggested based on their experimental results is

$$Nu_{nf} = 0.65 (Re^{0.65} - 60.22) (1+0.0169 Ø^{0.15}) Pr^{0.542} \quad (2.1)$$

The correlation for friction factor given by them is

$$f = 0.3164\ Re^{-.025} \left(\frac{\rho_{nf}}{\rho_{bf}}\right)^{0.797} \left(\frac{\mu_{nf}}{\mu_{bf}}\right)^{0.108} \quad (2.2)$$

Haghshenas Fard et al. (2010) did numerical study of Cu/water nanofluid flowing in a circular copper tube of 6mm diameter. Unstructured grid of 40 x 1400 is used. Laminar flow condition was considered. Both single and two phase models were used. Wall is maintained at a constant temperature. Velocity inlet and outlet flow boundary condition was given at inlet and outlet respectively. They observed that the heat transfer coefficient of the fluid increased with increase in nanoparticle concentration. They also found out that at higher Peclet number the increase in heat transfer coefficient is more significant compared to that at lower Peclet number.

Akbari et al. (2011) compared and analysed the results predicted by single phase and two phase models in CFD. Comparison was also made among different two phase models like volume of fluid, Eulerian and mixture models. Simulations were done in laminar flow regime having Reynolds number in the range of 1050 to 1600 for Al_2O_3- water nanofluid. Different volumetric concentrations of nanoparticle considered for the study were 0.6%, 1% and 1.6%. A horizontal tube having 0.0045m diameter and 0.97m length is considered as the geometry. Wall was subjected to uniform heat flux. Pressure-velocity coupling is done by SIMPLEC method. For discretization, second order upwind method is used. A 180 x 40 x 40 grid was used. They reported that the heat transfer coefficient results obtained by using single phase method were much lesser than those compared to the experimental results. In contrast, the results predicted by two phase models were very close to the experimental results. Therefore they concluded that the two phase models were more accurate. Also, they observed that results predicted by different two phase models were nearly same. But they recommend using volume of fluid (VOF) model since it is less expensive compared to other models. As the Reynolds number increased from 1050 to 1600, they observed an 11% overall increase in heat transfer coefficient.

Kalteh et al. (2011) numerically studied the effect of using Cu-water nanofluid in a microchannel. Eulerian two phase model was used for simulations. Simulations were carried out by taking different velocity and temperatures for the two phases. The 2-D geometry selected for this study was a parallel plate microchannel having a height of 200 µm and length 20 mm. Wall is maintained at a constant temperature of 303 K. At the inlet both the phases entered the microchannel with a uniform axial velocity. Outflow boundary condition is given at the outlet. SIMPLE method was incorporated for pressure velocity coupling. The

geometry was divided into a grid of 500 x 30. They observed that the difference in velocities of the two phases is very small in the entire flow field and the addition of nanoparticle is the reason for a small increase in hydrodynamic entrance length which in turn influences both the pressure drop and the heat transfer coefficient. They observed a slight increase in pressure drop with increase in nanoparticle concentration, at Re=1000 and at 1% volumetric concentration, the pressure drop was nearly 1.99% more than that compared to water. Also, the Nusselt number increased with increase in nanoparticle concentration but the increase in Nusselt number is more pronounced at lower Reynolds number. They also concluded that at lower concentrations, the diameter of nanoparticle has no significant effect on heat transfer.

Demir et al. (2011) numerically studied the effect of nanofluids on heat transfer when it flows through a double tube heat exchanger, using CFD. TiO_2-water nanofluid was considered. Single phase model was used for getting solutions. Nanofluids with nanoparticle concentration of 0.2%, 0.6%, and 1% were considered for numerical study. Nanofluid was assumed to be a single phase fluid with enhanced properties compared to that of base fluid. The numerical solutions were obtained using Fluent package in Ansys. SIMPLE method was used to couple the pressure and velocity. Pipe surface was maintained under constant heat flux of 10000 W/m^2. Grid size used was 1000 x 80. They observed that local heat transfer coefficient had higher slope at the pipe entrance region. They reported that as the concentration of nanoparticles and Reynolds number increases the pressure drop also increases, but, the difference in pressure drop between base fluid and nanofluid is very less at lower Reynolds number. Since the viscosity increases by adding nanoparticles to a base fluid, the wall shear stress also increases. Nusselt number and heat transfer coefficient increases with increase in Reynolds number and particle concentration.

Kamyar et al. (2012) have presented a research paper on application of computational fluid dynamics on nanofluids. They said that with the help of some slip mechanisms such as thermophoresis that lead to the increase in heat transfer, solving a two-phase model for a nanofluid has become easier. Two phase model gives accurate results compared to the single phase approach. They said that by considering the effect of Brownian motion and temperature dependency of viscosity and thermal conductivity could also enhance the accuracy of the results.

Kumar (2012) did a CFD study of heat transfer enhancement in pipe flow with Al_2O_3 nanofluid. He considered a circular pipe of diameter 0.017 m and 10 m length. The pipe was assumed to be perfectly smooth. Optimum mesh size was selected for both water and nanofluids. Mass, momentum and energy conservation equations were solved to carry out

steady state simulations. Turbulent flow was modelled using the RNG version of k-Ɛ viscous model. Base fluid considered was water at a temperature of 315 K. Velocity profile at the inlet was considered to be uniform. A constant wall temperature of 289 K was used at the wall boundary. Simulation was carried out using CFD solver FLUENT 6.3.26. Governing equations were solved using finite volume approach. He found out that, in turbulent flow regime, Nusselt number increased with increase in volume concentration of nanoparticles because of increase in thermal conductivity of the base fluid. He also showed that the increase in Nusselt number became more prominent at high Reynolds number. Nearly three times increase in Nusselt number can be observed at high Reynolds number. But, in case of laminar flow, Kumar (2012) showed that, for all volume fractions, the increase in Nusselt number is not as significant as in the turbulent flow. He said that single phase approach fails to predict the heat transfer in the laminar regime but the numerical prediction of Nusselt number using single phase approach in turbulent flow regime agrees well with the experimental results.

Keshavarz Moraveji et al. (2012) compared the single phase and two phase approach in CFD. CFD modeling of laminar forced convection on Al_2O_3 nanofluid with size particles equal to 33 nm and particle concentrations of 0.5, 1 and 6 wt.% within 130<Re<1600 in mini-channel heat sink is executed by four individual models. They found out that deviation from experimental with two phase modeling is less than that of single phase. Also Difference among three two phase models is very narrow but considering less run time and CPU usage, mixture model is better.

Keshavarz Moraveji et al. (2012) conducted numerical investigation of Al_2O_3/ water nanofluid inside a circular tube using both single phase and two phase models. Nanoparticle concentrations of 1% and 4% were considered. Simulations were carried out at various Reynolds number (250, 500, 750, 1000). Geometry considered is a two dimensional pipe having 1 m length and 10 mm diameter. At the wall, constant heat flux boundary condition with heat flux of 5000 W/m^2 is used. At the inlet they have assumed uniform axial velocity and temperature. First order upwind scheme is used. Velocity pressure coupling was done by SIMPLE procedure. Unstructured grid of 400 x 10 is considered. They observed that at 1% concentration, there is a difference of nearly 10% between the results obtained using single phase and two phase models. They also found out that as the concentration increases the difference starts decreasing. They also gave a correlation for Nusselt number in a horizontal function which is given below.

$$Nu = 0.716\ Re^{0.314}\ Pr^{0.6}\ Ø^{0.3} \quad (2.3)$$

Darzi et al. (2013) conducted experiments to see how addition of Al_2O_3 nanoparticles to water affects the performance of a heat exchanger. Their experimental setup included a double tube heat exchanger having copper inner tube of 8.1 mm diameter and a steel outer tube of 150 mm diameter. The length of the heat exchanger was 220 cm. Experiments were carried out for various concentrations of nanoparticles (0.25%, 0.5%, 1%) and at different Reynolds number (between 5000 and 25000). They found out that heat transfer rate increases with increase in nanoparticle concentration and Reynolds number, but they suggested that the increase in heat transfer rate mainly depends on concentration of nanoparticles rather than Reynolds number. Also, they suggested that the decrease in laminar sub-layer thickness at higher Reynolds number is one of the reasons for increase in heat transfer rate. Friction factor also increases with increase in nanoparticle concentration, but, the increase in heat transfer rate is more predominant.

Sekhar et al. (2013) investigated the behaviour of convective heat transfer and friction factor of Al_2O_3 nanofluids. To do this they considered a horizontal circular tube with twisted tape arrangement. The circular tube was subjected to constant heat flux boundary conditions. The tube was made of copper and was of size 0.012 m diameter same as the riser tube in solar flat plate collector. To obtain constant heat flux, the copper tube was heated uniformly by wrapping it with nichrome heaters having maximum rating of 1000 W. The tube was made of copper and was of size 0.012 m diameter same as the riser tube in solar flat plate collector. Experimental setup included a chiller, collecting tank, and storage connected to a pump. Nanofluids at different volume concentrations used in the experiment were 0.02, 0.1 and 0.5%. They showed that the heat transfer coefficients enhances with the use of nanofluids, especially in the entrance region. At particle concentration of 0.5% and twisted tape having ratio X/D=10, the local heat transfer coefficient was observed to increase up to 26% compared to water in a tube. Also, they found out that the Nusselt number increases with increase in Reynolds number and particle concentration. The increase in Nusselt number for the nanofluid compared with water is of the order of 8-12% for all the particle volume concentrations. Also, they showed that friction factor increases with increase in particle concentration while it decreases with increasing Reynolds number. Friction values of nanofluid, compared to that for water, are more due to increase in viscosity of fluid and decrease in Reynolds number.

Ghozatloo et al. (2014) conducted experiments to determine the behaviour of graphene nanofluid based on water in the entrance region. Laminar conditions were considered with the concentrations of suspensions being 0.05, 0.075, 0.1% by weight of alkaline grapheme oxide in water was used. The flow circuit consisted of a pump, a tank and a cooling system and the test section which is composed of a horizontal circular copper tube of inside and outside diameter 1.07 cm and 1.3 cm respectively and of 1 m length. To obtain constant heat flux, the copper tube was heated uniformly by wrapping it with nichrome heaters. To get laminar flow of fluid volumetric flow rate of fluid used was 0.8 lit/min. They found out that thermal conductivity of the samples increases with increase in concentration up to certain limit, but starts decreasing later on. In the experiment they conducted they observed that at 25^0C with addition of 0.05, 0.075 and 0.1% (wt) of grapheme in water, the thermal conductivity increased by 15%, 29.2% and 12.6% respectively compared to that of base fluid. They clearly indicated through graphs that with increase in temperature and concentration of nanofluid, the local heat transfer coefficient also increases. By adding only 0.05% (wt) of graphene to water they observed an increase in heat transfer coefficient of 7.2% compared to that of base fluid.

Delavari and Hassan Hashemabadi (2014) in their numerical stud**y** simulated heat transfer in nanofluids. They considered Al_2O_3 nanoparticles in water and ethylene glycol based fluid. They considered both laminar and turbulent flow regime in a flat tube. They used both single phase and two phase approaches for simulation. Laminar flow was considered was considered for nanofluids based on ethylene glycol and turbulent flow was considered for water based nanofluid with concentrations varying for both nanofluids from zero to 1% for alumina particles. Half of a flat tube of an air cooled heat exchanger was considered as computational domain because of symmetry. Since fluid bulk heat transfer is high near the wall, cell density near the wall was taken more. They showed that for pure water at an inlet temperature of 50^0C and a Reynolds number of 9500 the locally averaged skin friction factor and heat transfer coefficients decreased as the boundary layers develop along the length of the tube. Also, Nusselt number and local surface friction factor for both the water based and ethylene glycol based nanofluid increased uniformly with increase in particle concentration and Reynolds number. But pressure drop increases with increasing particle concentration.

Kulkarni et al. (2014) have presented a research paper on application of nanofluids in heating buildings. The experimental setup used by them for this purpose consisted of a pump, heat transfer test section, a counter flow heat exchanger, flowmeter, differential pressure transducer, bypass valve, reservoir and several data loggers. The heat transfer test

section is a tube made up of copper with diameter 3.37 mm and 1 m length. Constant heat transfer boundary condition was maintained. Base fluid used was 60:40 ethylene glycol/water. Nanoparticles considered were of CuO, Al_2O_3 and SiO_2. They conducted viscosity tests on nanofluid and determined that the nanofluid behaves as a Newtonian fluid. The viscosity of the nanofluid at certain temperature increases with increasing volume concentrations. They also found out by viscosity tests that nanofluid viscosity is very high at lower temperatures and it decreases exponentially with increase in temperature. They showed that the heat transfer increases with increase in Reynolds number and the heat transfer coefficient increases with increase in particle concentrations. Among CuO, Al_2O_3 and SiO_2 nanofluids, CuO nanofluids have highest enhancement in heat transfer coefficient. Also, the CuO nanofluids have highest viscosity and density and hence have higher pressure loss. They also conducted an analysis of energy required for cold climate building. They observed pumping power savings by using nanofluids. From their experiments it was evident that the pumping power savings are 11.7% for CuO nanofluid, 27.6% for the SiO_2 nanofluid and 38.3% for the Al_2O_3 nanofluid.

Madhesh et al. (2014) conducted experimental investigation on convective heat transfer and rheological characteristics of Cu-TiO_2 hybrid nanofluids. Their test section consists of concentric tubes of length 1.8 m. Outer diameters of inner and outer tubes are 6.4 mm and 12.7 mm respectively and the tubes were of 1mm thickness. The hybrid nanocomposite considered had an average size of 55 nm. They suggested that copper nanoparticles acted as extended surfaces on the titania nanoparticles. Due to this, a generation of a network of thermal interfaces are formed between their grain boundaries and layers of fluidwhich results in increase in thermal conductivity compared to just TiO_2 nanoparticles. They showed that with increase in nanocomposite volume concentration and its temperature, the thermal conductivity of the hybrid nanofluid increases because of Brownian motion and a decrease in thermal boundary layer thickness. They showed through their experiments that tut 52% and 49% increase in both convective heat transfer coefficient and Nusselt number respectively by addition of volume proportions up to 1% nanofluid compared to that of base fluid. The reason for this increase in heat transfer characteristics, as they said, was mainly due to improved thermal conductivity of these particles and reduction in thermal resistance at wall surface of the inner tube. Though there was an increase in pressure drop and friction factor with increase in volume concentration of nanoparticles, the increase in heat transfer characteristics overshadowed them. They also provided a new correlation for Nusselt number

as a function of Reynolds number, Prandtl number and volume concentration of hybrid nanocomposite which is given below,

$$Nu=0.012* Re * Pr^{0.333} * Ø^{0.032} \quad (2.4)$$

This equation, as they indicated, was valid under the flow field with 4000 < Re < 8000 and volume concentrations ranging from 0.1% to 2.0%.

Esfe et al. (2014) conducted experiments to find out heat transfer characteristics of COOH functionalized multi-walled carbon nanotubes (CNTs) with water as base fluid. They said that the thermal conductivity of d fluid with CNTs increases with increase in temperatures due to breaking down of agglomeration between the nanoparticles which in turn results in uniform dispersion of CNTs in water. From their experiments they found out that the higher thermal conductivity of multi-walled carbon nanotubes compared to water is one of the main reasons for increase in heat transfer. They observed an increase in Nusselt number by 41% for 1% concentration and the corresponding increase in heat transfer coefficient is 83%. But the pressure drop also increased by 37% compared to the base fluid at same concentration.

Azmi et al. (2014) did Experimental determination of heat transfer coefficients of TiO_2/water nanofluid up to 3% volume concentration flowing in a circular tube is undertaken. The investigations are conducted in the Reynolds number range of 5000 to 25000 at a bulk temperature of 30^0C. They found out that the heat transfer enhancement is inversely increased with twist ratio. Also they observed that the value of heat transfer coefficient of TiO_2 /water nanofluid evaluated at the same concentration is 11.4% greater than water for twist ratio five.

Vahid Delavari et al. (2014) did CFD simulation of turbulent and laminar flow heat transfer in nanofluids passing through flat tube using CFD for single phase and two phase approaches Concentrations of 0.1,0.3,0.5,0.7 and 1% by volume of Al_2O_3 nanoparticles in water and ethylene glycol. They predicted that Nusselt number increased uniformly as Reynolds number and concentration of nanoparticles is increased. Also Brownian motion decreased the boundary layer thickness, increasing heat transfer and friction factor increase with increase in nanoparticle concentration

Davarnejad et al. (2015) conducted the CFD simulation of heat transfer characteristics of a nanofluid in a circular tube using Fluent software (version 6.3.26). They considered laminar flow and constant heat flux as boundary condition. Al_2O_3 nanoparticles in water with concentrations of 0.5%, 1.0%, 1.5%, 2% and 2.5% were used in this simulation. Two particle sizes with average size of 20 and 50 nm were used in this research. The pipe used in the simulation was of 1 m length and had 6 mm inner diameter. Single phase

approach was used for the simulation of behaviour of nanofluid. The main aim of the simulation was to find out effect of nanoparticle concentrations on the convective heat transfer coefficient. Reynolds number considered was in the range of 700 to 2050. GAMBIT was used to generate geometry and grid which is an integrated pre-processor for CFD analysis. 20 meshes were considered in radial direction having size ratio of 1 from centre to the wall. Further they used 1000 meshes in horizontal direction. They showed the variation of heat transfer coefficient in the tube with velocity for various concentrations of nanoparticles with diameters of both 20 and 50 nm. According to them, increasing the volume fraction and velocity, results in increase in heat transfer coefficient. They showed that heat transfer coefficients increased by decreasing the diameter of the particle and increasing the velocity of fluid flow. The average heat transfer coefficient and Nusselt number also increases with increase in particle concentrations and flow rate. Also, particles with lesser diameter have high heat transfer, i.e. 20 nm particles shows maximum heat transfer.

Sun et al. (2015) recently experimented on Fe_2O_3-water nanofluids. Their test section was made up of copper and inner grooved copper tubes. They measured differential pressure of Fe_2O_3 water nanofluid at different Reynolds number for both the tubes and found out that inner grooved copper tube had high pressure drop and it increased with increase in Reynolds number. Also at 0.4% concentration nanofluid they observed that there was an increase in heat transfer coefficient by 33.52% when compared to that of base fluid. The groove in the tube increased the intensity of turbulent flow thus helping in further enhancing heat transfer coefficient value.

Ahmed et al. (2015) studied the laminar heat transfer and fluid flow characteristics in an equilateral triangular duct using combined vortex generator and nanofluids. Distilled water based Al_2O_3 and SiO_2 nanofluids with concentrations of 0.5% and 1% were used. They conducted experiments in Reynolds number range of 500-1500. They observed that Maximum heat transfer enhancement obtained is around 31.87% and 33.22% for alumina oxide and silica oxide nanofluids, respectively when VG and nanofluids are used simultaneously.

Mahdavi et al. (2015) did CFD analysis on vertical tube of ID 4.5 mm and length 1 m by using DPM and mixture model with water based Al_2O_3 nanofluid under laminar flow regime. Heat transfer coefficient and pressure drop both increases with increase in nanoparticle concentration.

Davarnejad et al. (2015) did Computational fluid dynamics modeling of Magnesium oxide-water nanofluid. The volumetric concentrations of nanoparticles in base fluid considered for simulations were 0.0625%, 0.125%, 0.25%, 0.5%, 1%. Simulations were

conducted for the Reynolds number range of 3000 – 19000. Their geometry was two dimensional having 15 cm in radial direction and 252 cm length. The geometry was generated using GAMBIT software. Velocity inlet and pressure outlet was selected for tube inlet and outlet boundary condition respectively. No slip condition was given to the wall. The wall is maintained at constant temperature of 313.15 K. A grid of 15 x 252 meshes was used. For pressure velocity coupling, SIMPLE algorithm was used. Models used were single phase, VOF and mixture models. Turbulence model used was K-ε turbulence model. They observed increase in Nusselt number and friction factor with increase in nanoparticle concentration. Also, results obtained using the VOF and mixture models were found to be closer to the experimental results as compared to the results obtained using single phase model.

Navaei et al. (2015) did numerical study to investigate the effects of nanofluid on heat transfer coefficient in a rib-grooved channel. Nanoparticles considered were Al_2O_3, SiO_2, ZnO and CuO. These nanoparticles were dispersed in different base fluids like water, ethylene glycol and glycerine in different proportions ranging from 1 to 4%. Uniform heat flux boundary condition was used at the wall. The RNG k-ε turbulence model was used. The pressure velocity coupling was done using SIMPLE algorithm. Among the different rib shapes (rectangular, spherical and trapezoidal), they found out that spherical shaped ribs gave highest Nusselt number. Also they found out that heat transfer rate of glycerine-SiO_2 nanofluid is higher than others. They noted that with change in parameters like volume concentration of nanoparticles, nanoparticle diameter, there is no significant changes in skin friction coefficient, whereas, the Nusselt number increases with increase in nanoparticle concentration.

Aghaei et al. (2015) did a numerical study on Al_2O_3 – water nanofluid flowing through a tube. They carried out simulations in turbulent flow regime with different Reynolds number ranging from 10000 to 100000. Different diameters of nanoparticles used were 25, 33, 75, and 100 nm. Volumetric concentrations of nanoparticles considered were 0.001, 0.01, 0.02, 0.03 and 0.04. 2-D geometry of tube having length 1 m and diameter 0.02 m was used. At the wall, constant temperature of 310 K was used. Velocity inlet boundary condition was used at the inlet with fluid having uniform axial velocity at inlet and temperature of 300 K. The nanofluid was considered to be in single phase. K-ε model was used for turbulence. Coupling of pressure - velocity is done using SIMPLE algorithm. They observed that Nusselt number increases with increase in Reynolds number and volumetric concentrations. They also asserted the fact that random motion is one of the important reasons for heat transfer augmentation. They observed that at higher Reynolds number (Re > 60000); the turbulence in

the flow field has more effect on Nusselt number and pressure drop than the concentration of nanoparticles.

Zhao et al. (2016) did numerical investigation of laminar heat transfer and flow characteristics of Al_2O_3–water nanofluids through a flat tube at constant heat flux boundary condition. They observed that Al_2O_3–water nanofluids have higher heat transfer coefficient and pressure drop than base fluid.

Chapter 3

Research Gap and Objective

3.1 Research Gap

1. The use of turbulators with nanofluids as the heat exchanger fluid in a double tube heat exchanger is relatively new area. Hence, more research is needed to understand the heat transfer characteristics and the parameters that affect the heat transfer characteristics in these.
2. The numerical study using CFD tools like ANSYS Fluent for investigation of heat transfer characteristics in a heat exchanger with nanofluid as heat exchanger fluid is mainly done by considering simple wall boundary conditions like constant heat flux or constant wall temperature. Since, in many of the practical applications of heat exchanger these conditions do not exist there is a need to consider wall boundary conditions other than this.

3.2 Objectives

The main objective of the present study is to conduct experimental and numerical investigation of performance characteristics of double tube heat exchanger. Study is conducted at different flow rates. Following are the set of objectives considered for this thesis.

1. To investigate experimentally the effect of using TiO_2-H_2O nanofluids (at a volumetric concentration of 0.05% and 0.026%) as heat exchanger fluid.
2. To investigate the performance of heat exchanger with twisted tapes of twist ratio 3.2, 4 and 5, when both water and nanofluid is used as heat exchanger fluid. The nanofluid under consideration for experimental purpose is TiO_2-water nanofluid with concentrations of 0.05% and 0.026%. The different twist ratios of twisted tape used include 3.2, 4 and 6.

3. To conduct numerical investigations using ANSYS Fluent 14.5 to study the effect of nanofluids on performance of the heat exchanger. Also, to compare the single phase and two phase model approaches for nanofluids.
4. To numerically investigate the effect of different nanoparticles, nanoparticle concentration and nanoparticle size. 1% volumetric concentrations of Al_2O_3, TiO_2 and CuO in water is considered for this study. To study the effect of nanoparticle size, TiO_2 nanoparticles of size 30 nm and 50 nm are considered.

Chapter 4

Preparation of Nanofluid

Nanofluid is prepared by dispersing solid particles of nanosize in a base fluid like water ethylene glycol etc. Usually nanofluids are prepared by either one step method or two step method. One step method involves making and dispersing of the nanoparticles in a base fluid at the same time and two step method involves production of nanoparticles and later on dispersing it in a base fluid. The commonly used method between the two is two step method, hence two step method is used for preparing the nanofluid.

The synthesis of nanoparticles is beyond the scope of this thesis. Hence, nanoparticles are procured first and then dispersed in a base fluid here. The percentage concentration of nanoparticle by weight to be added is decided before the preparation. Based on the concentration decided the amount of nanoparticle to be added to the base fluid is calculated by using the formula given below.

$$f_v = \frac{V_{np}}{V_{bf}+V_{np}} \tag{4.1}$$

Figure 4.1: Chemical balance apparatus.

The weight of the nanoparticle to be added is measured by using chemical balance shown in the image above. Properties of the nanoparticle considered for both experimentation and simulation are given in Table 4.1. Table 4.2 shows the amount of nanoparticle used.

Table 4.1: Properties of nanoparticles considered for experimentation and simulation

Nanoparticle	Density (kg/m^3)	Specific heat (J/kgK)	Thermal conductivity (W/mK)
TiO_2	4230	692	8.4
Al_2O_3	3960	773	40
CuO	6000	551	33

Table 4.2 Amount of nanoparticle to be taken per litre of water

Nanoparticle Concentration (percentage)	Amount of nanoparticle per litre of water
0.05	2.11 gm
0.026	1.1 gm

The preparation of nanofluid mainly involves operating the fluid with dispersed solid particles in two apparatus, namely,

1. Magnetic Stirrer.
2. Ultrasonic vibrator.

4.1 Magnetic Stirrer

The nanoparticles in the fluid should be dispersed properly. This can be done by using magnetic stirrer. Nanoparticles of required weight are mixed in the deionised water in a flask. A magnetic bead is placed in the flask. After mixing, the flask is placed on disk provided on the magnetic stirrer. A magnetic stirrer has a magnetic base, the speed of which can be controlled using dimmer provided on the apparatus. The magnetic bead used in the flask is of different magnetic pole than the magnetic base provided on the magnetic stirrer. Hence, when the magnetic stirrer is switched on, the magnetic bead present inside the flask starts rotating. Due to the rotation of the magnetic bead inside the flask, the nanoparticles present in the fluid are dispersed. Magnetic stirrer is shown in the Figure 4.2.

Figure 4.2: Magnetic stirrer

In spite of magnetic stirring of the nanofluid, there is a chance that nanoparticles in the fluid will agglomerate. Hence, to ensure that there is no agglomeration of nanoparticles, surfactants are added to the fluid. Murshed et al. (2008) suggested that, for the TiO_2-water nanofluid, cetyltrimethyl ammonium bromide (CTAB) surfactant is the best. Duangthongsuk and Wongwises (2009) also suggested using CTAB surfactant but with very low concentration (0.01%) to ensure that the surfactant added do not affect the nanofluid's thermophysical properties. Hence, very low concentration of CTAB surfactant was added during the magnetic stirring process. Magnetic stirring is done for about 30 min.

4.2 Ultrasonic Vibrator

Even after stirring in magnetic stirrer, there is a chance that, after sometime, the nanoparticles in the nanofluid may form clusters or undergo sedimentation. Hence, to avoid this, the stirred nanofluid is operated in an ultrasonic vibrator. Bath type sonicator is used for this purpose. Figure 4.3 and 4.4 shows an image of ultrasonic vibrator (sonicator).

Figure 4.3: Ultrasonic Vibrator

After stirring, the nanofluid sample is placed in this ultrasonic bath type sonicator for about 1 hour at room temperature. Ultrasonic vibrator breaks any clusters formed and ensures that the particles in the fluid are in the dispersed state. Figure 4.5 shows the image of the nanofluid prepared.

Figure 4.4 Ultrasonic Vibrator

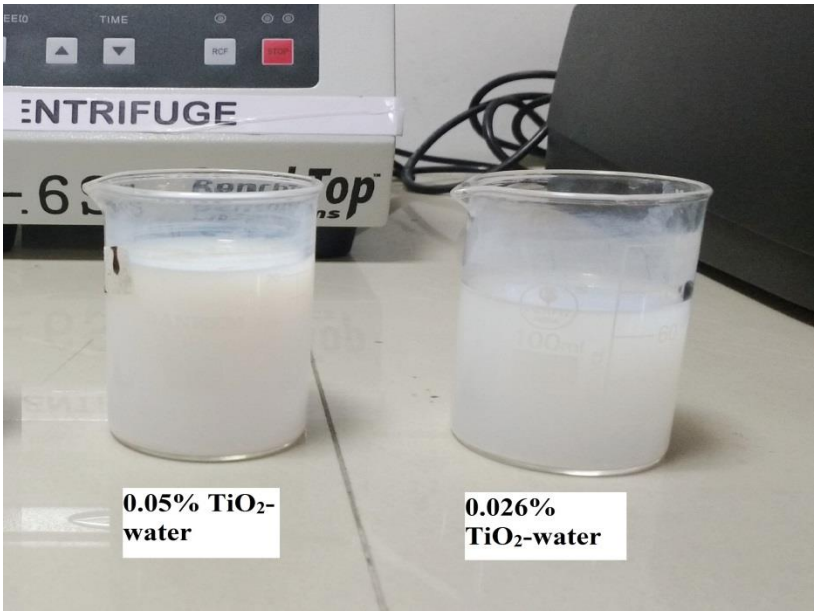

Figure 4.5: Nanofluid prepared

Chapter 5

Experimental Setup and CFD Methodology

5.1 Experimental Setup

A double tube heat exchanger is used as a test section for conducting experiments. Figure 5.1 shows an image of the setup used for experimental purpose. Figure 5.2 shows schematic diagram of the setup.

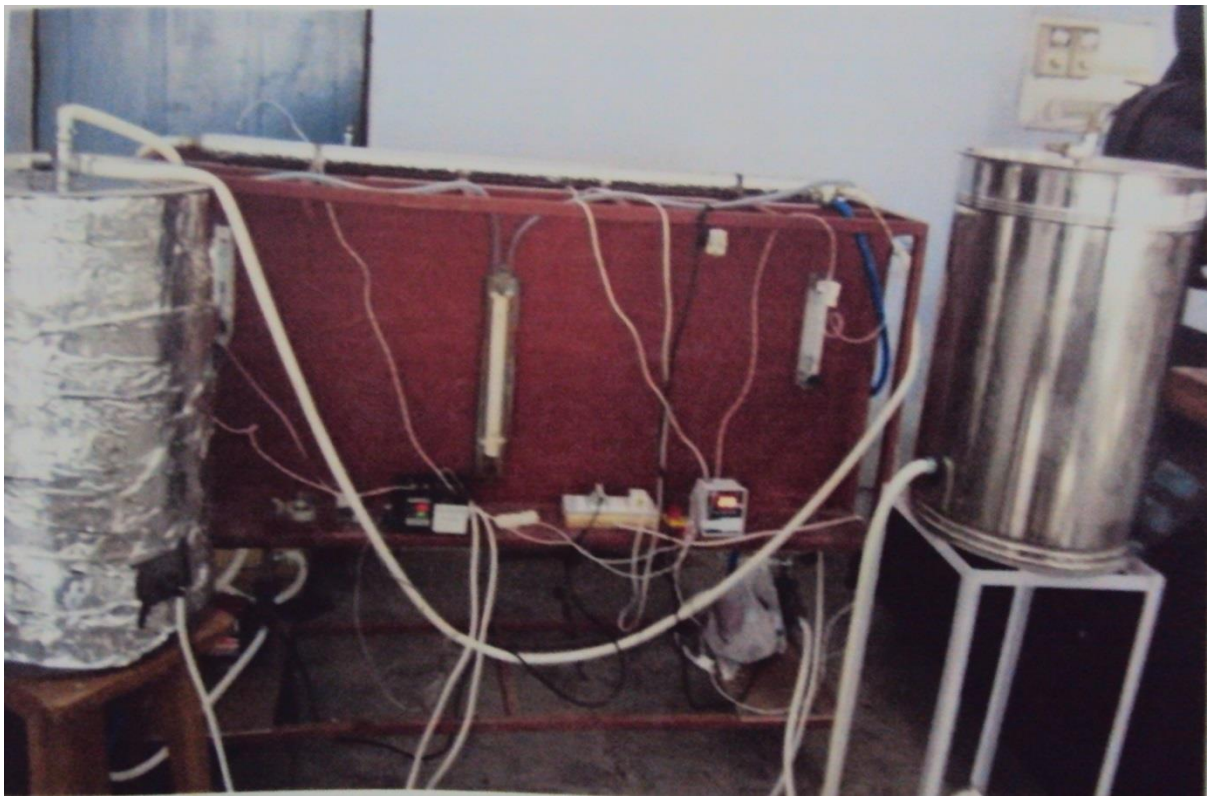

Figure 5.1: Experimental setup

The experimental setup includes following important components,

1. A double tube heat exchanger is used for finding out the heat transfer and the parameters that affect heat transfer between hot and cold fluids. The inner tube of a double tube heat exchanger is made up of copper since it has higher thermal conductivity.
   Inner diameter of copper tube: 12 mm

   Inner tube thickness: 2 mm

   The outer tube is made of galvanized iron.

Outer diameter of galvanized iron tube: 25.4 mm

Outer tube thickness: 3 mm

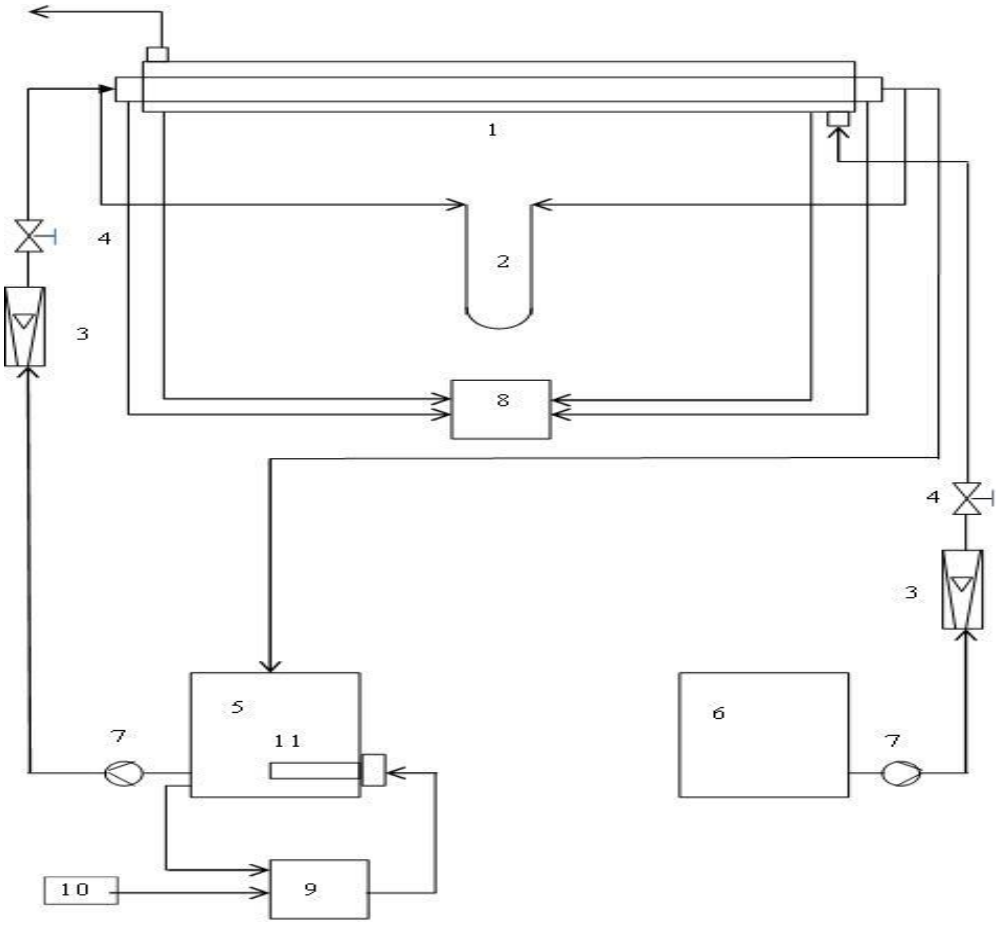

Figure 5.2: Schematic diagram of Experimental setup (1) Test section (2) Manometer (3) Rotameter (4) Control valve (5) Hot water tank (6) Cold water tank (7) Pump (8) Digital panel meter (9) PID controller (10) Power Supply (11) Heater

The outer galvanized iron tube is also insulated with asbestos tape to avoid heat loss by convection to the surroundings. Also to minimize heat losses due to radiation, the outer tube is covered with aluminium tape. Figure 5.3 shows an image of double tube heat exchanger used for the experimental purpose.

2. As shown in figure, two water tanks are used. One for hot water and the other for cold water. The hot water tank is covered by asbestos sheet and an aluminium tape to reduce both convection and radiation losses. The hot water tank is provided with a heater

element of 3 KW power to heat the fluid used. The fluid from the hot water tank is fed to the inner tube and is circulated back to the hot water tank.

Figure 5.3: Double tube heat exchanger

3. Pumps are used to feed hot and cold water tank to inner and outer tube, respectively. Figure 5.4 shows the image of the pump used.

4. Rotameters are used to measure the flow rate of fluid going to the heat exchanger. Two separate rotameters are used for measuring flow rate of hot and cold fluid. Control valves are provided on both the rotameters to regulate the flow of fluid into the system. Through this required flow rate of the fluid can be set for carrying out experiments. Figure 5.5 shows an image of rotameter used in the setup.

Figure 5.4: Centrifugal Pump

Figure 5.5: Rotameter

Figure 5.6: PID controller.

5. Since the hot fluid is circulated back to the tank, the temperature of the fluid inside the tank changes. To avoid this and to maintain constant temperature of the hot fluid a Proportional Integral Derivative (PID) controller is used. A PID controller consists of a temperature sensor, a temperature display with a provision to set the required temperature and a power input control. The temperature sensor of the PID controller is immersed in the hot fluid. The sensor sends the temperature feedback signal to the device, based on which the power input is either switched on or off. The power supply will be switched off

only if the temperature of the fluid crosses the set temperature. Figure 5.6 shows an image of the PID controller used.

6. Temperature sensors are used to measure temperature at different points in the double tube heat exchanger. The temperature sensors used here is PT100 thermocouples. The temperature sensors are placed at 4 different points, namely, the inlet and outlet of inner tube and the inlet and outlet of the outer tube. The readings from all the temperature sensors are displayed on a digital panel meter. The temperature at the required point can be noted by operating the selector switch present on the digital panel meter. Figure 5.7 shows the image of the digital panel meter used in the experiment.

Figure 5.7: Digital panel meter

Figure 5.8 U-tube mercury manometer

7. Nanofluid is used as hot fluid. Since the main aim of the experiment is to study the effect of the adding nanoparticles to the fluid, the pressure difference is measured between the inlet and outlet of the inner tube where hot fluid flows. Two tapping, one at the inlet and other at the outlet of the inner tube, are taken and connected to the two sides of the U-tube mercury manometer to measure the pressure difference between the two points.

Figure 5.9: Making of twisted tape on lathe.

8. The heat transfer can also be enhanced by passive techniques. Passive technique involves the use of any turbulators like springs, twisted tapes, twisted wire brushes etc., which disturbs the flow which in turn results in the heat transfer enhancement. The twisted tapes are used in this experiment. Twisted tapes of different twist ratios are used.

   Twisted tapes are made by fixing both the ends of a GI sheet (10 mm width and 1.5 m length) on the lathe and turning at very low speed. This is done till the required pitch or twist ratio is achieved. The twisted tape is then inserted in the inner tube of the double tube heat exchanger. Figure 5.9 shows the image of the twisted tape being made on the lathe. The twist ratios used for the current study are 3.2, 4 and 6.

Figure 5.10: Twisted tape being inserted into the inner tube

5.2 CFD Methodology

CFD is used to solve and analyse fluid flow and heat transfer problems. The steps followed in CFD analysis is

1. Geometry modelling to define the geometry or the region on which CFD analysis is to be carried out.
2. Mesh generation where the geometry defined is divided into grids.
3. Setting up boundary conditions and selecting the governing equations to be used.
4. Solving the governing equation. In this step the governing equation is first converted into integral equation which is then converted into system of linear algebraic system.
5. Post processing is done to visualize and analyse the results obtained using CFD

Geometry modeling was done using Design Modeler in Ansys 14.5. The geometry defined here is similar to the one used in the experimental setup. Therefore the dimensions of the geometry are as follows:

1. Inner tube inner diameter: 12 mm
2. Inner tube thickness: 2 mm
3. Outer tube inner diameter: 25.4 mm
4. Outer tube thickness : 3 mm

Meshing was done in Ansys Fluent 14.5. The geometry is divided into number of grids. The details of the mesh are given below.

1. Meshing method used:- Automatic

2. Meshing size taken:- 5 mm
3. Number of inflation layers used:- 5 (programme controlled method)
4. Number of elements: 7643350
5. Average Orthogonal quality of mesh: 0.845
6. Average Skewness : 0.25 (generally should not exceed 1 for a good quality mesh)

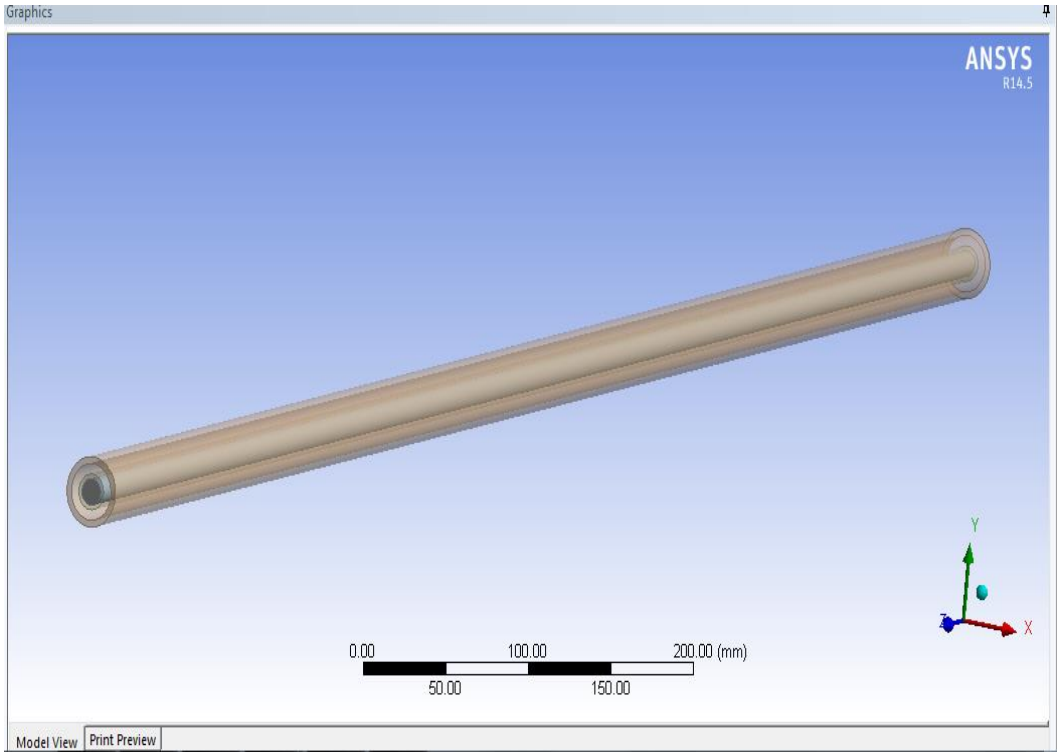

Figure 5.11: Modeling of double tube heat exchanger in Design modeler 14.5.

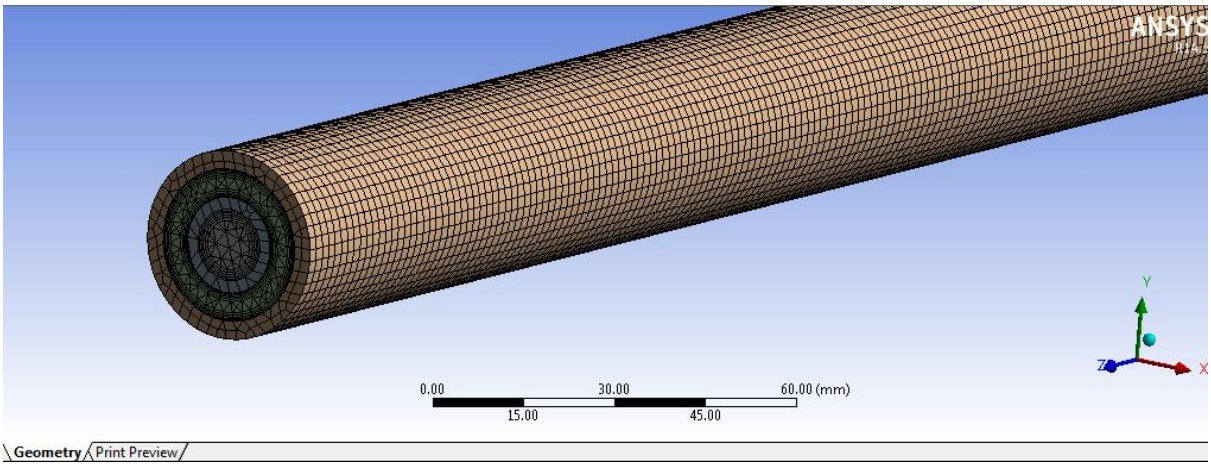

Figure 5.12: Meshing of double tube heat exchanger.

Figure 5.11 shows the modelling of double tube heat exchanger. Figure 5.12 shows the how the geometry defines is divided into number of grids. Since the effect of boundary layer is found only in immediate vicinity of walls, we need to have more

number of grids near the wall. Therefore, inflation layers are added near the wall of the tubes to capture the boundary layer effects near the walls. Skewness of the mesh denotes the quality of the mesh used. In general the skewness of the mesh should not exceed more than 1 for a good quality mesh. Average skewness in this is 0.25 and maximum is 0.893. The setup used in the Ansys Fluent 14.5 is tabulated below.

Table 5.1: ANSYS Fluent setup.

Steps	**Selections**
Model	Energy equation ON Viscous :- RNG K-ε model Single phase.
Materials	Fluid- Water, solid- Steel and Copper
Inlet	Velocity Inlet (for hot water) 1. 0.4174m/s (Re-5000) 2. 0.8348m/s (Re- 10000) 3. 1.2522m/s (Re- 15000) 4. 1.6696m/s(Re-20000) 5. 2.087m/s (Re-25000) Temp- 333K Velocity Inlet (for cold water): 0.986m/s Temp-300K gauge pressure zero
Outlet	Pressure outlet, gauge pressure zero
Wall	No slip condition, Stationary wall. Heat flux zero.

The analysis is done for different inlet velocities of hot water depending upon the Reynolds number taken during the experiments. The inlet velocity of cold water is kept same throughout the analysis. The inlet temperature of hot water is set to 333K (60^0C) which is also the same set during experiments.

Table 5.2: For two phase model

Steps	**Selections**
Model	Energy equation ON Viscous :- RNG K-ε model Multiphase model: Mixture model
Materials	Water – primary phase TiO_2 nanoparticle- secondary phase Solid- Steel and Copper
Inlet	Velocity Inlet (defined separately for water and TiO_2 phases) 1. 0.4174m/s (Re-5000) 2. 0.8348m/s (Re- 10000) 3. 1.2522m/s (Re- 15000) 4. 1.6696m/s(Re-20000) 5. 2.087m/s (Re-25000) Temp- 333K (For mixture) Velocity Inlet (for cold water): 0.986m/s Temp-300K gauge pressure zero TiO_2 concentrations of 0.05%, 1%, 2% and 3%.
Outlet	Pressure outlet, gauge pressure zero
Wall	No slip condition, Stationary wall. Heat flux zero.

Table 5.2 shows the setup conditions used in ANSYS Fluent 14.5 for solving nanofluid flow problem using two phase model. The boundary condition is same as that for single phase except that mixture model is used. Water is selected as the primary phase and TiO_2 nanoparticles as secondary phase. The properties of TiO_2 nanoparticles are available from the literature study and are input into the setup.

The coupling of pressure and velocity is done by using Couple method. The pressure discretization is done using PRESTO scheme. The first order upwind scheme is used for discretization of momentum, energy, turbulent kinetic energy and turbulent dissipation rate.

5.3 Data Reduction

The heat transfer rate of hot fluid and cold fluid is given by.

$$Q_h = m_h C_{ph}(T_{h_i} - T_{h_o}) \quad (5.1)$$

$$Q_c = m_c C_{pc}(T_{c_o} - T_{c_i}) \quad (5.2)$$

Where, Q and m denotes heat transfer rate and mass flow rate, respectively. The subscripts h and c denotes hot and cold fluid, respectively.

The average heat transfer rate is given by

$$Q_{ave} = \frac{Q_h + Q_c}{2} \quad (5.3)$$

The heat transfer coefficient is calculated by,

$$h_i = \frac{Q_{ave}}{A_i * LMTD} \quad (5.4)$$

Where, Logarithmic Mean Temperature Difference (LMTD) is given by

$$LMTD = \frac{\left(T_{h_i} - T_{c_o}\right) - (T_{h_o} - T_{c_i})}{\ln \frac{\left(T_{h_i} - T_{c_o}\right)}{(T_{h_o} - T_{c_i})}} \quad (5.5)$$

Where, subscripts i and o denote inlet and outlet of tube, respectively.

The friction factor is given by,

$$f = \frac{2 * D * \Delta P}{\rho L V^2} \quad (5.6)$$

Where, D is the diameter of the tube, ΔP is the pressure difference between inlet and outlet of the tube, L is length of the tube and V is inlet velocity of the fluid.

Chapter 6

Results and Discussions

6.1 Experimental Results

The results from the experiment need to be validated using the standard correlations available. If the difference in the results obtained by experiment and correlations are in an acceptable range then the setup can be considered as reliable. For the setup used, validation is done by comparing the values of heat transfer coefficient and friction factor obtained from the experiment with those obtained using standard correlations by considering water as the heat transfer fluid. The standard correlation provided by Dittus-Boelter and Naphon et al. [2006] is used for validating heat transfer coefficient values. For validating the friction factor values correlations given by Blasius and Naphon et al. [2006] is used. The equations are given below.

Dittus-Boelter equation for calculating Nusselt number in turbulent flow regime for internal flow is given by,

$$\mathrm{Nu} = 0.023\mathrm{Re}^{0.8}\mathrm{Pr}^{0.4} \tag{6.1}$$

Naphon et al. gave correlations for calculating the Nusselt number and friction factor for Reynolds number ranging from 5000 to 2500 when a double tube heat exchanger is used and is given by,

$$\mathrm{Nu} = 1.84(\mathrm{Re} - 1500)^{0.32}\mathrm{Pr}^{0.07} \tag{6.2}$$

$$\mathrm{f} = 0.66\mathrm{Re}^{-0.33} \tag{6.3}$$

Blasius equation for calculating friction factor for internal flow under turbulent flow regime is given by,

$$\mathrm{f} = 0.3164\mathrm{Re}^{-0.25} \tag{6.4}$$

Figure 6.1 and 6.2 shows the comparison between experimental and theoretical heat transfer coefficient and friction factor values, respectively. It can be seen from the graph that the difference between experimental and theoretical values is very less. The difference lies in

the range of 10% to 15% for heat transfer coefficient and less than 11% for friction factor as compared to Naphon et al. [2009].

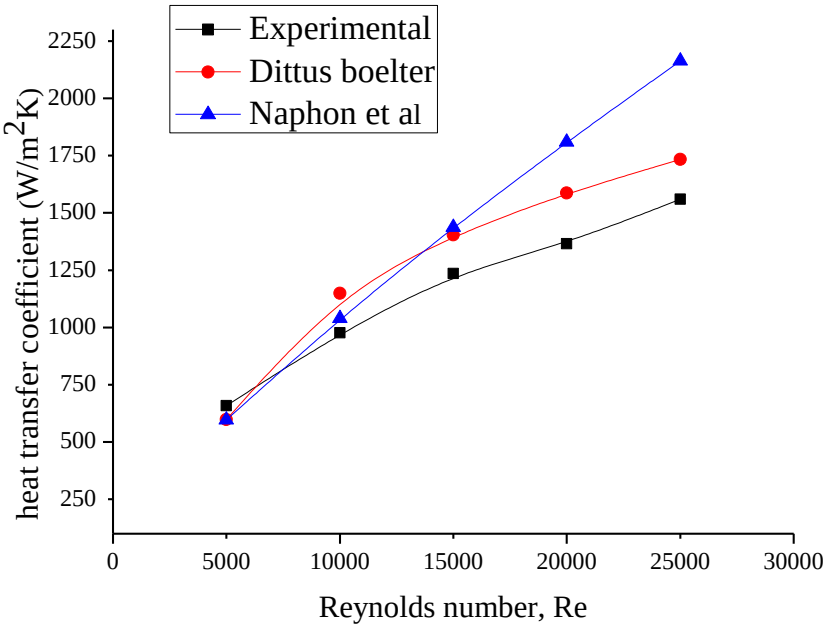

Figure 6.1: Comparison of experimental heat transfer coefficient with standard correlations.

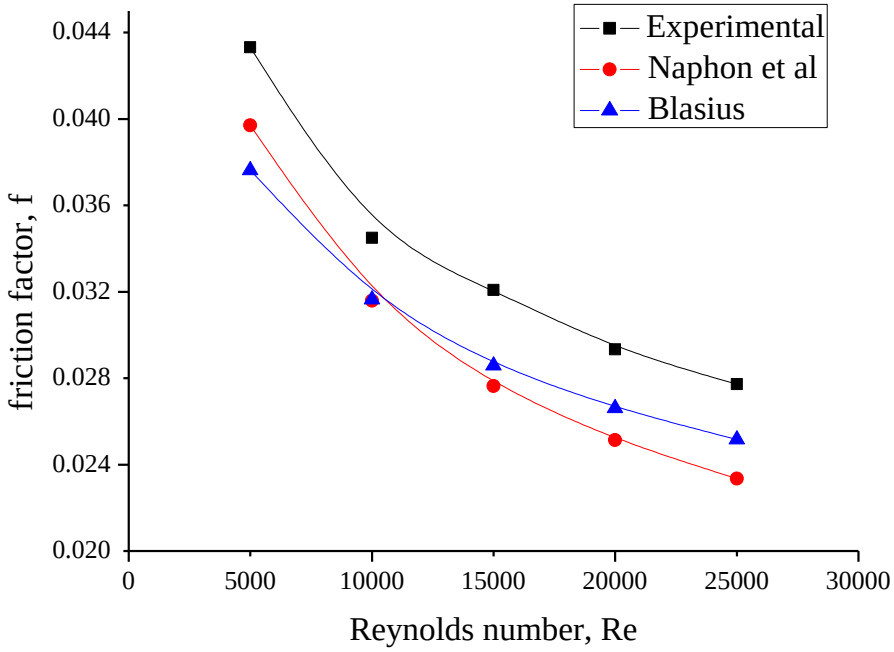

Figure 6.2: Comparison of friction factor.

6.1.1 Effect of Inserting Twisted Tape in a Double Tube Heat Exchanger

Heat transfer coefficient can be increased by passive methods. Passive methods include using corrugated tubes instead of simple tube, inserting twisted tapes, and springs etc. into a tube. Among these passive methods, inserting a twisted tape method is used majorly because of it has simple configuration and it is easy to install. Insertion of twisted tapes results in effective mixing of fluid in central and near wall region which results in increase in heat transfer coefficient. Also, because of this induced turbulent fluctuation the boundary layer thickness decreases helping in achieving improvement in heat transfer.

Figure 6.3 shows the effect of inserting twisted tape into the tube on heat transfer coefficient. It can be seen from the graph that heat transfer coefficient increases by using twisted tape. Twisted tapes of different twist ratios (y_0/W) have been investigated. From the graph it is observed that the heat transfer coefficient increases with decrease in twist ratio. The maximum increase in heat transfer coefficient is observed for twist ratio of 3.2 and the increase is in the range of 1.34 - 1.36 times as compared to the heat transfer coefficient of plain tube.

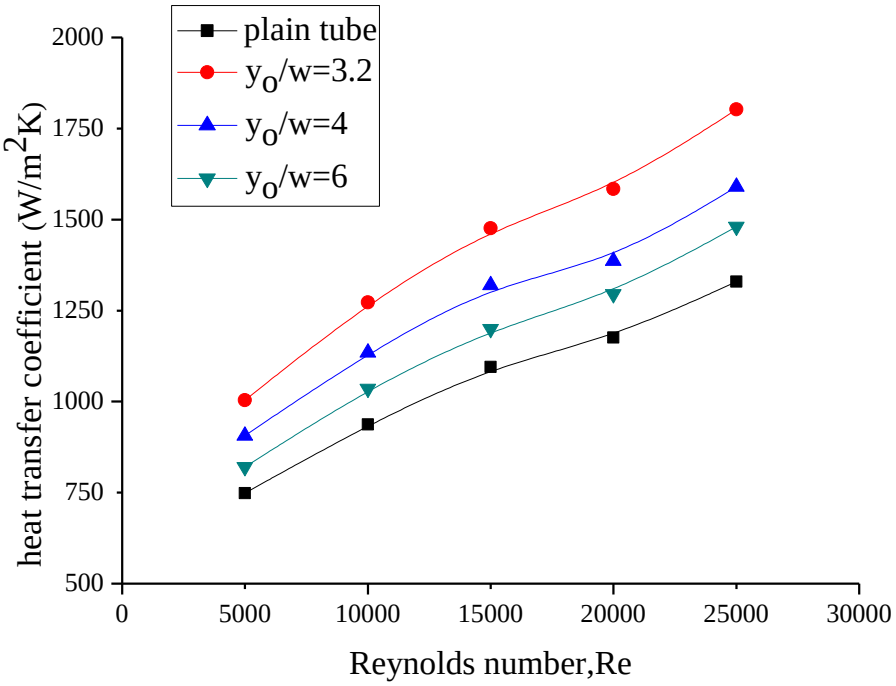

Figure 6.3: Variation of heat transfer coefficient with different twist ratios

Along with the increase in heat transfer coefficient, the insertion of twisted tape also results in increase in pressure drop. This results in increase in friction factor and hence,

power required for pumping. Figure 6.4 shows the variation of friction factor with different twist ratios. It is observed from the graph that friction factor increases with decrease in twist ratio and decreases with increasing Reynolds number. The friction factor for twist ratio of 3.2 is 2.1 times that of simple tube. The nature of the graph obtained for heat transfer coefficient and friction factor is same as those obtained by Halit Bas and Veysel Ozceyhan [2012].

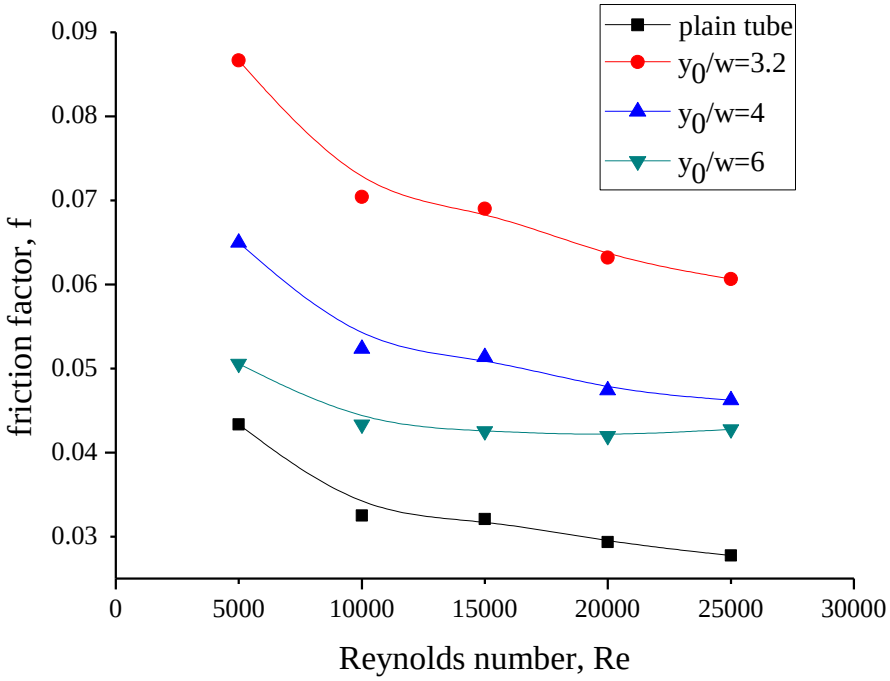

Figure 6.4: Variation of friction factor with twist ratio

Though the pressure drop and pumping power increases, the insertion of twisted tape in the tube is advantageous. This can be shown by a factor called thermal performance factor, which is given by,

$$\eta = \left(\frac{h_t}{h_p}\right)\left(\frac{f_p}{f_t}\right)^{1/3} \quad (6.5)$$

Where h and f represent heat transfer coefficient and friction factor, respectively. The subscripts p and t represents values for plain tube and tube with twisted tape, respectively. Thermal performance factor represents the ability of an enhanced heat exchanger to increase heat transfer rate at same pumping power. Figure 6.5 shows the variation of thermal performance factor with different twist ratio.

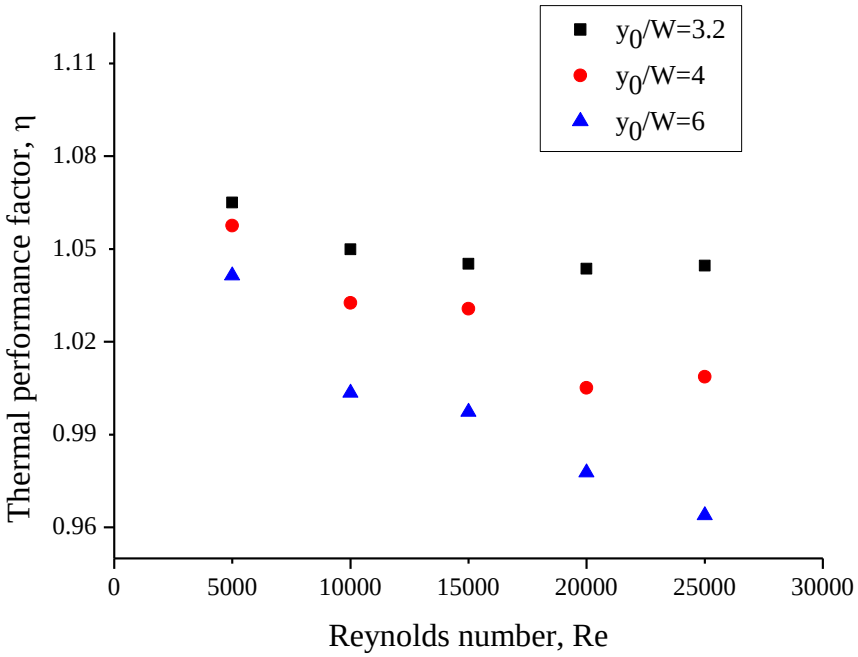

Figure 6.5: Variation of Thermal performance factor with twist ratio

6.1.2 Effect of Addition of TiO_2 Nanoparticles to Water.

Addition of nanoparticles to the base fluid such as water results in increase in heat transfer coefficient. This can be attributed to the facts that the addition of nanoparticles results in increase in thermal conductivity and Brownian motion. Experiment has been conducted with TiO_2 nanoparticle concentrations of 0.05% and 0.026%. Figure 6.6 shows the effect of addition of nanoparticles on heat transfer coefficient. The graph shows that the heat transfer coefficient increases with the addition of nanoparticle compared to water and it increases with increase in concentration of nanoparticle.

The friction factor of the nanofluid used in the experiment is nearly same as that of water since the concentration of nanoparticle used for the experiments is very less. This can be verified by Duangthongsuk and Wongwises [2009] who conducted experiments with 0.2% volumetric concentration of nanoparticle and found out that the friction factor values of nanofluid coincide with that of water. Figure 6.7 shows the variation of friction factor with nanoparticle concentration and Reynolds number.

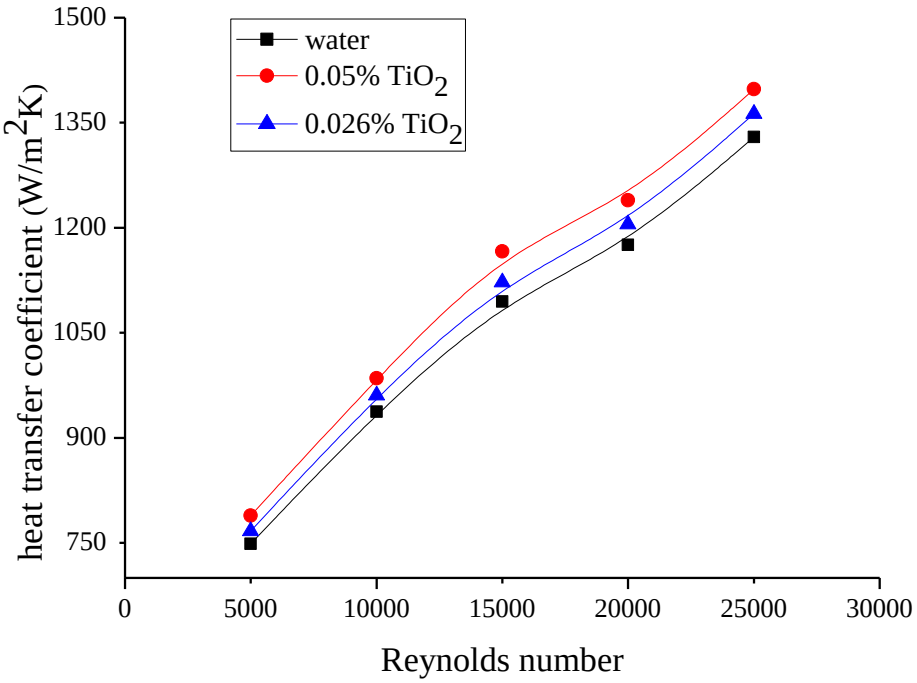

Figure 6.6: Heat transfer coefficient variation with nanoparticle concentration

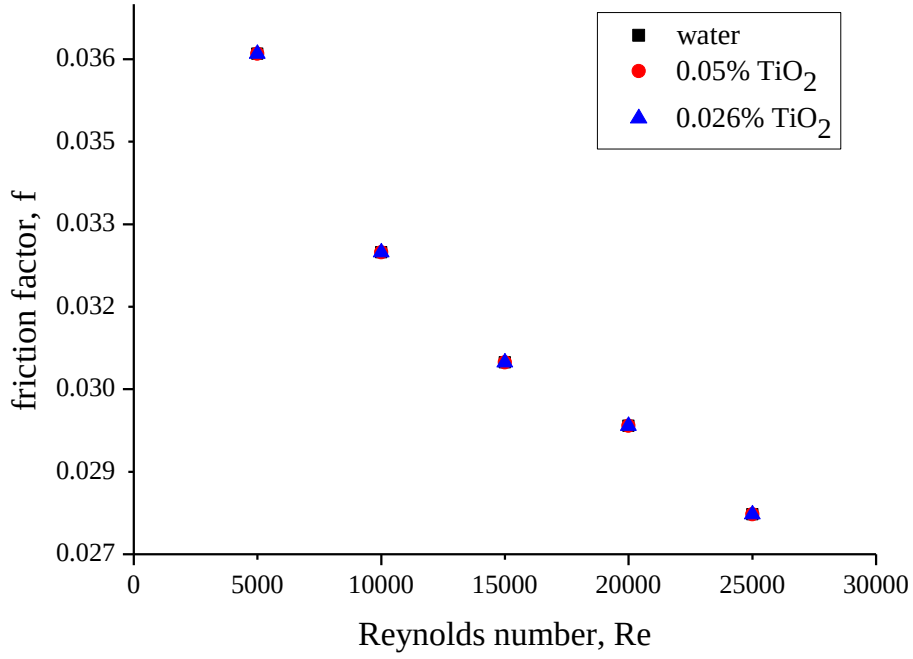

Figure 6.7: Friction factor variation with nanoparticle concentration

6.1.3 Effect of Using Twisted Tape with Nanofluids as Working Fluid

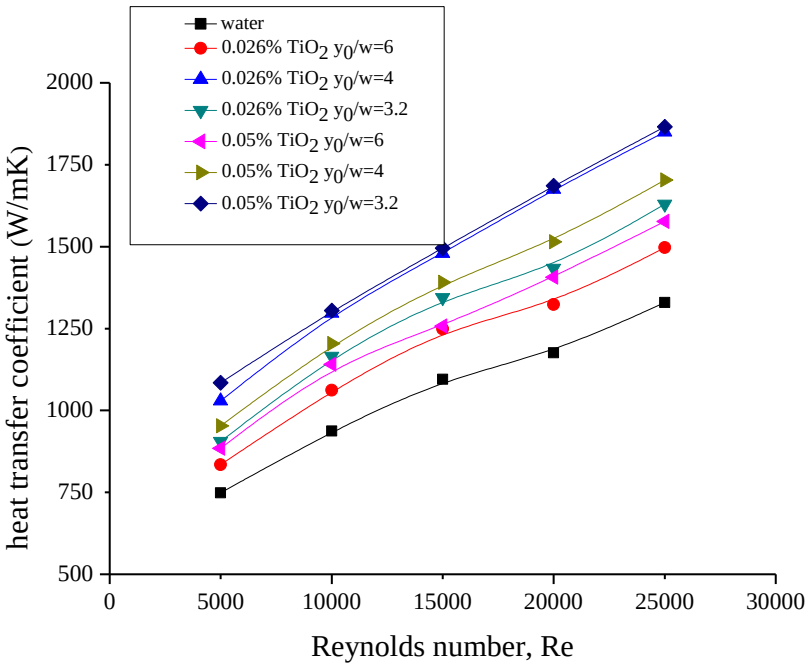

Figure 6.8: Heat transfer coefficient for various TiO_2 concentrations and twist ratios.

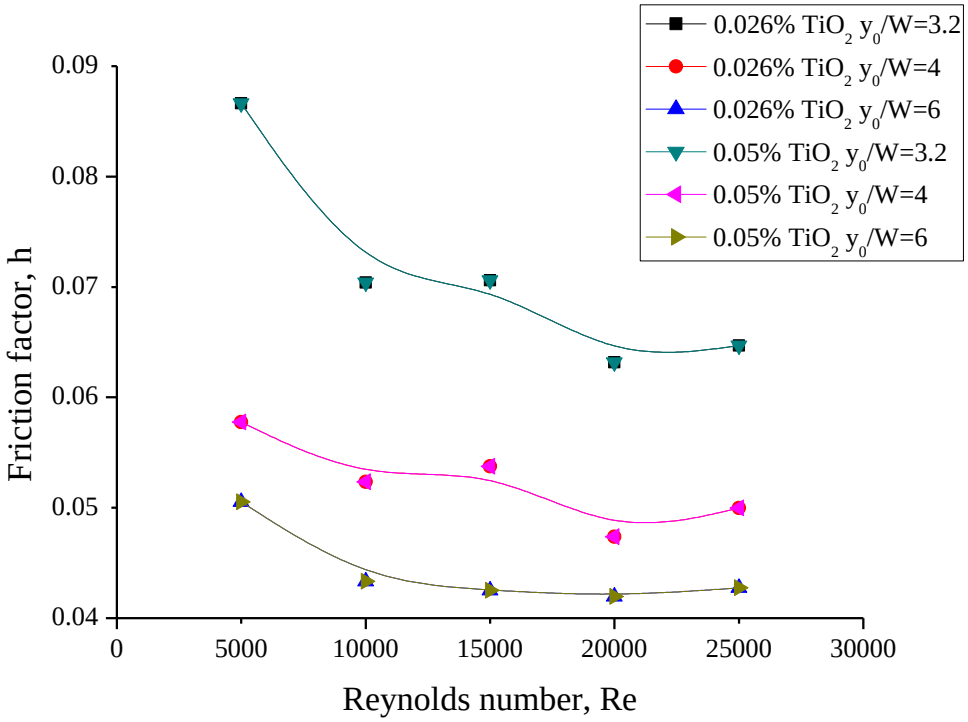

Figure 6.9: Friction factor variation for different nanoparticle concentration and for different twist ratios of twisted tape.

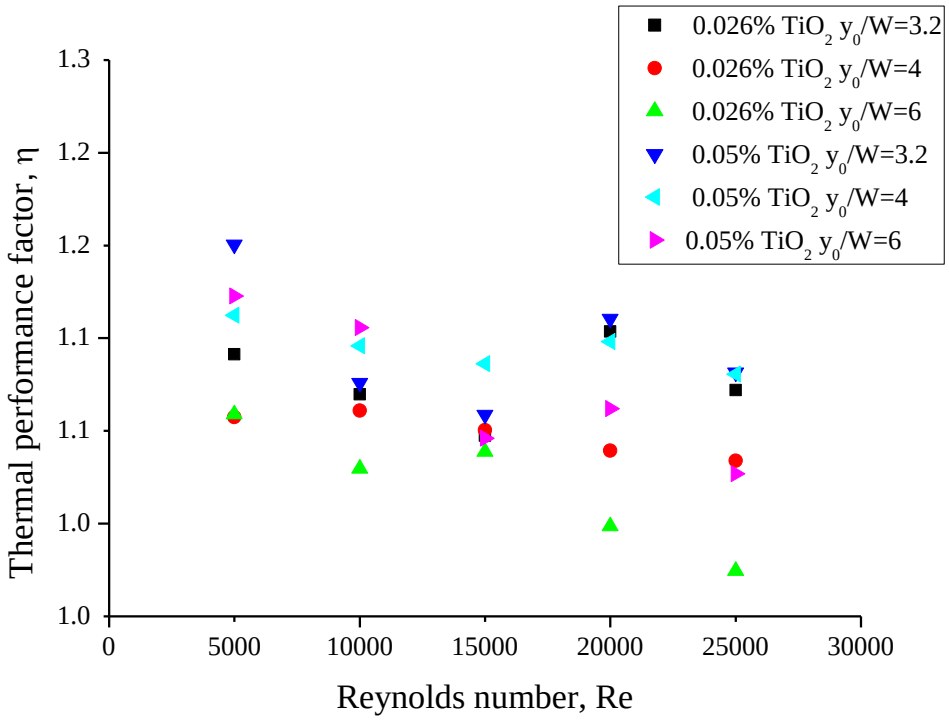

Figure 6.10: Variation of thermal performance factor for different concentration of nanoparticle and different twist ratios of twisted tape.

The effect of using nanofluid as heat exchanger fluid with twisted tape inserts has been investigated in the present study. The heat transfer coefficient and the friction factor increases with the use of nanofluid in a tube with twisted tape inserts. For 0.05% TiO_2-water nanofluid and twist ratio of 3.2, the heat transfer coefficient increase is upto 1.45 times that obtained when water is used in plain tube. When twisted tapes are used with water as working fluid, the enhancement was about 1.34 times the plain tube with water. Friction factor increase is found to be 2.1 to 2.2 times. Figure 6.8 and 6.9 shows the variation of heat transfer coefficient and friction factor for various nanoparticle concentration and twist ratios. Figure 6.10 shows the thermal performance factor variation.

6.2 CFD Results

6.2.1 Comparison of CFD and Experimental Results

The results obtained by CFD simulations are prone to errors and are never fully reliable. Hence, the results obtained from CFD simulations need to compared and validated with the results obtained from experimentation

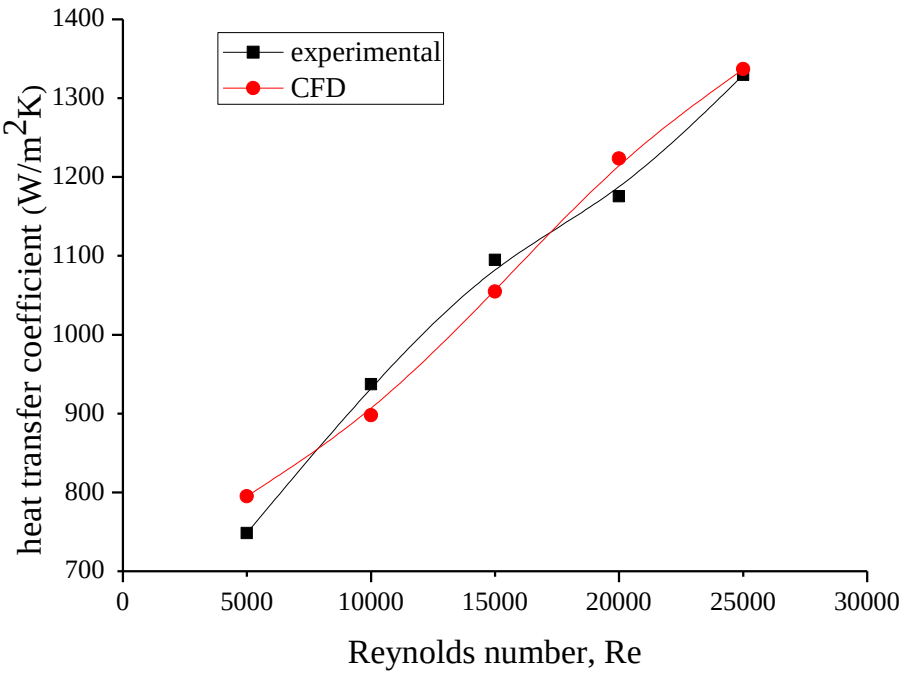

Figure 6.11: Comparison of heat transfer coefficient values obtained from CFD and experiments

Figure 6.11 shows the heat transfer coefficient variation with Reynolds number with water as the working fluid. It can be seen from the graph that the CFD results are comparable with the experimental. The maximum deviation in heat transfer coefficient values got by simulations is 6% from experimental results. Hence the simulated results are reliable in the present study.

Figure 6.12 shows the temperature profile showing how the temperature of both hot and cold water varies along the length of the double tube heat exchanger. Since this is a counter flow heat exchanger the temperature of the hot fluid decreases in one direction which can be seen in the Figure 6.12 where the colour of inner hot fluid changes from red to orange. Similarly in the opposite direction in the outer tube, the temperature of cold water is increasing which is indicated by colour change from blue to cyan. The scale of temperature variation is shown at the top left corner of the image.

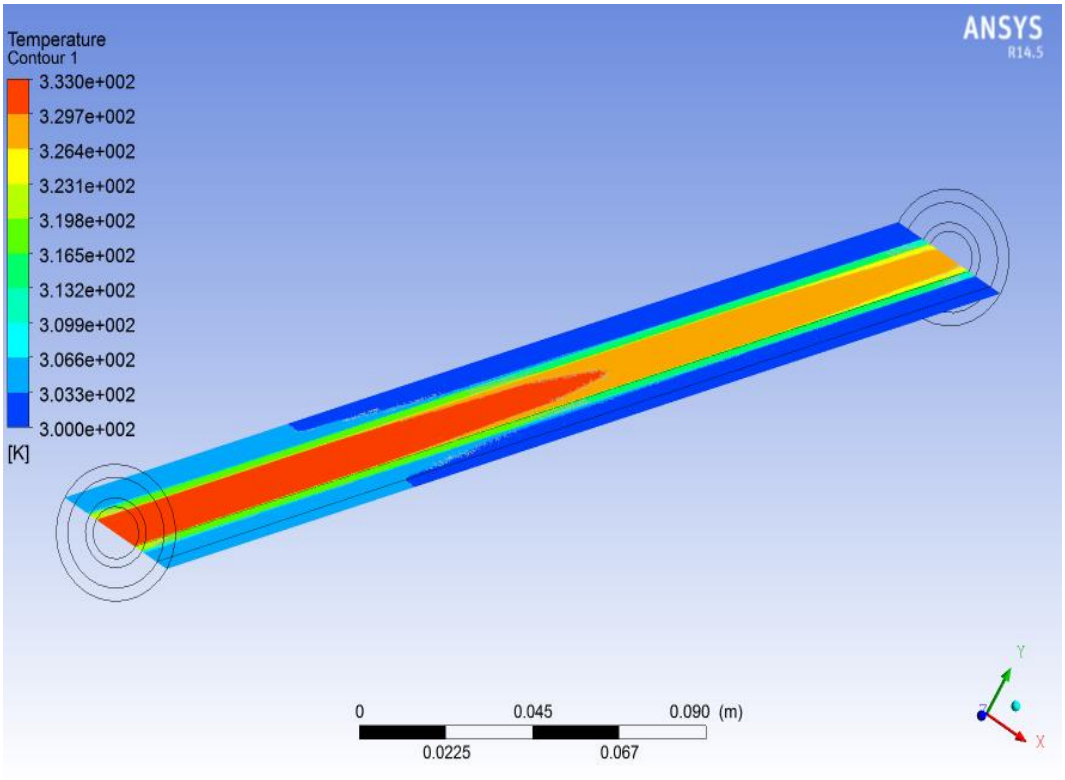

Figure 6.12: Temperature variation of hot and cold water along the length of double tube heat exchanger.

6.2.2 Comparison of Single Phase and Two Phase Models

Nanofluid is prepared by dispersing solid particles in a base fluid. In ANSYS Fluent a nanofluid flow problem can be approached in two ways. First approach is by treating the nanofluid as a single phase fluid with change in properties according to the concentration used. Second approach is by treating nanofluid as a two phase fluid. Figure 6.13 shows the comparison of heat transfer coefficient values obtained by experiments, single phase CFD model and two phase CFD model. There are different two phase models but mixture model is used in the present study.

It can be seen from the graph that the results obtained using two phase models is more nearer to the experimental then the single phase model. The maximum deviation from the experimental results is found to be 5.9% and 11% for two phase and single phase models respectively. Hence, two phase model gives more accurate results for a flow problem involving nanofluids.

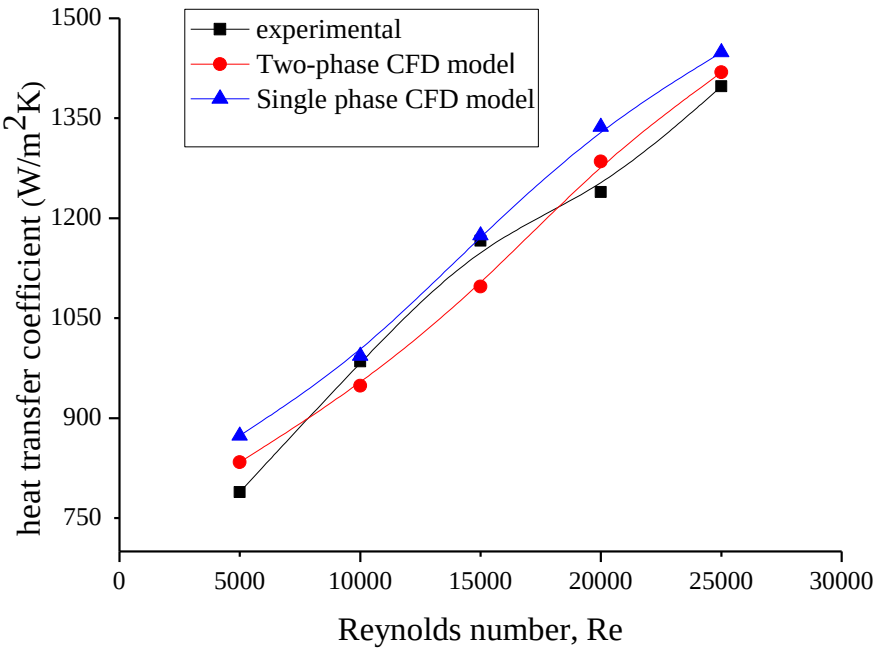

Figure 6.13: Comparison of single phase and two phase CFD models.

6.2.3 Numerical Study of Effect of change in Nanoparticle Concentration on Performance of Heat Exchanger

It is evident from the experiments that due to the addition of nanoparticles there is an increase in heat transfer coefficient. Also, from the previous sections it can be inferred that the results obtained for nanofluid flow using two phase model in ANSYS Fluent 14.5 is nearer to that of experimental results. Hence, the numerical results are reliable. Therefore, further parametric variations can be done in ANSYS Fluent 14.5. Figure 6.14 shows the variation of heat transfer coefficient with increase in volumetric concentration of nanoparticles in water. It can be observed from the graph that the heat transfer coefficient increases with addition of more and more nanoparticle. This can be attributed to the fact that addition of nanoparticle results in increase in thermal conductivity of the fluid. Also, addition of nanoparticle induces Brownian motion which results in decrease in boundary layer thickness and hence results in increase in heat transfer coefficient. TiO_2-water nanofluid with nanoparticle concentrations of 0.05%, 1%, 2% and 3% is considered in this study.

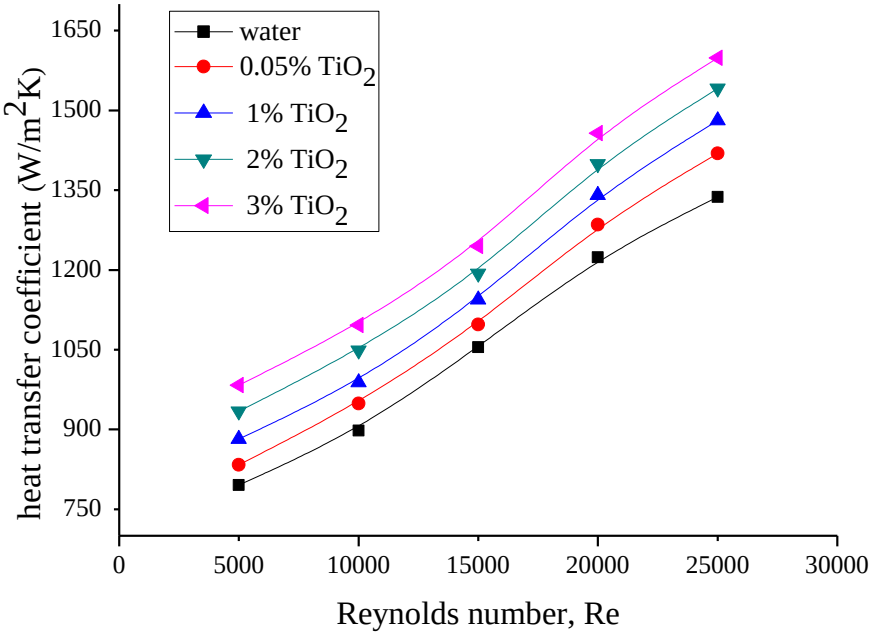

Figure 6.14: Variation of heat transfer coefficient with nanoparticle concentration

The maximum increase in heat transfer coefficient is 6%, 10.9%, 17.4% and 23.4% for TiO_2-water nanofluid with TiO_2 concentrations of 0.05%, 1%, 2% and 3%, respectively.

Figure 6.15 shows the variation of surface heat transfer coefficient along the length of the tube for various TiO_2 concentrations. It can be seen from the graph that the length of the tube after which the heat transfer coefficient starts decreasing with a nearly constant slope increases with increase in nanoparticle concentration. This infers that the entrance length, which is the length of the pipe after which velocity profile is fully developed, increases with increase in nanoparticle concentration. Hence, the average heat transfer coefficient also increases since the heat transfer coefficient is maximum in the entrance length region of the pipe.

Figure 6.16 shows the variation of wall shear stress along the length of the tube. It can be seen from the graph that the shear stress increases with increase in concentration and decreases along the length of the tube.

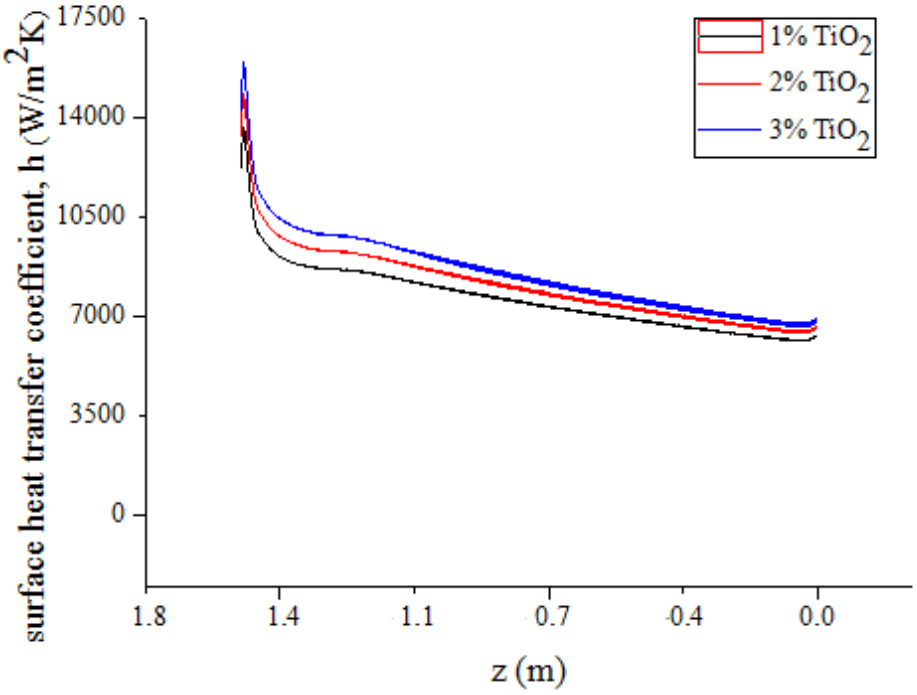

Figure 6.15: Variation of surface heat transfer coefficient along the length of the tube

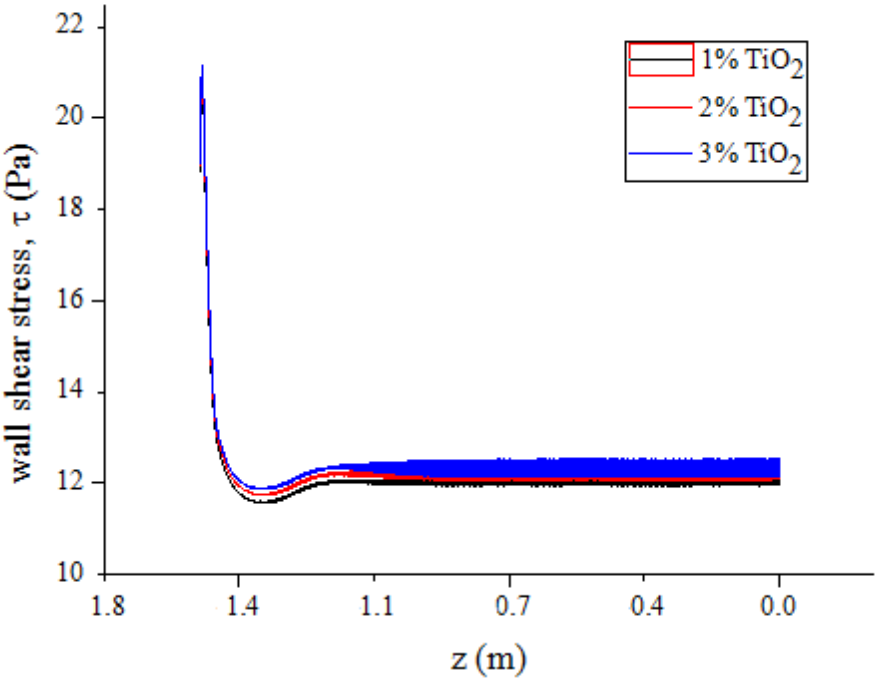

Figure 6.16: Variation of wall shear stress along the length of the tube

6.2.4 Effect of Different Nanoparticles on Heat Transfer Coefficient

Figure 6.17 shows the variation of heat transfer coefficient for different nanoparticles at different Reynolds number. Nanoparticles under consideration are TiO_2, Al_2O_3 and CuO nanoparticles. Volumetric concentration of 1% is used in the study. Among the three nanoparticle considered, Al_2O_3-water nanofluid shows maximum increase in heat transfer coefficient since the thermal conductivity of Al_2O_3 nanoparticle is more than the other nanoparticles considered. The increase in heat transfer coefficient is in the range of 9-11%, 20-27% and 21-30% for TiO_2-water, Al_2O_3-water and CuO-water nanofluid, respectively.

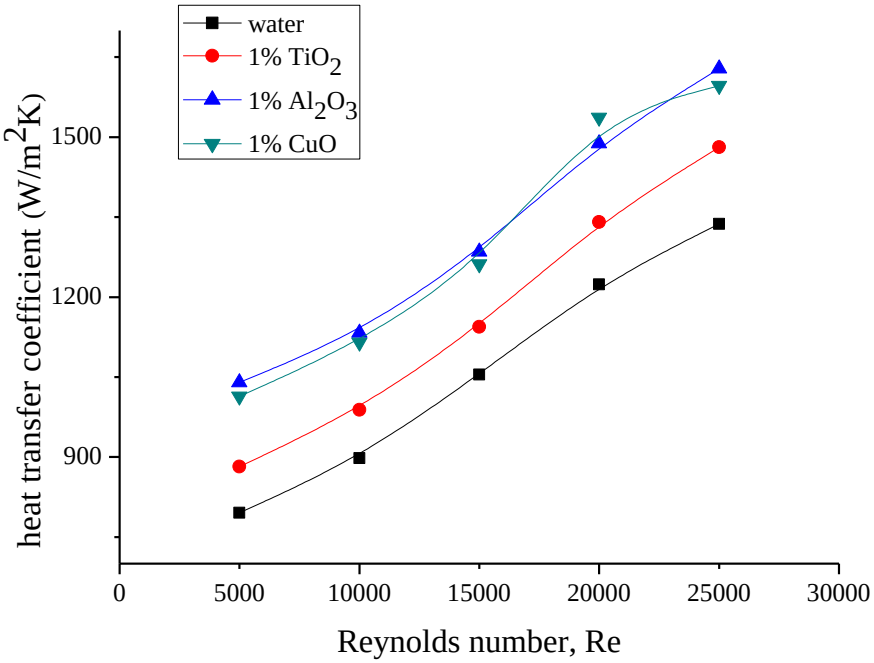

Figure 6.17: Variation of heat transfer coefficient for different nanoparticles.

6.2.5 Effect of Nanoparticle Size on Heat Transfer Coefficient

Figure 6.18 shows the heat transfer coefficient values for nanoparticles with different diameters. Nanoparticles of size 30 nm and 50 nm are considered for simulations. It can be inferred from the graph that there is no difference in the heat transfer coefficient values for both the diameters considered. This is because the volumetric concentration used is very less (0.05%). Vajjha et al. [2010] conducted experiments with different SiO_2 nanoparticle sizes. In their experiments they observed that at 2% SiO_2 concentration and for nanoparticle sizes of 20 nm, 50 nm and 100 nm, there is no difference in heat transfer coefficient values.

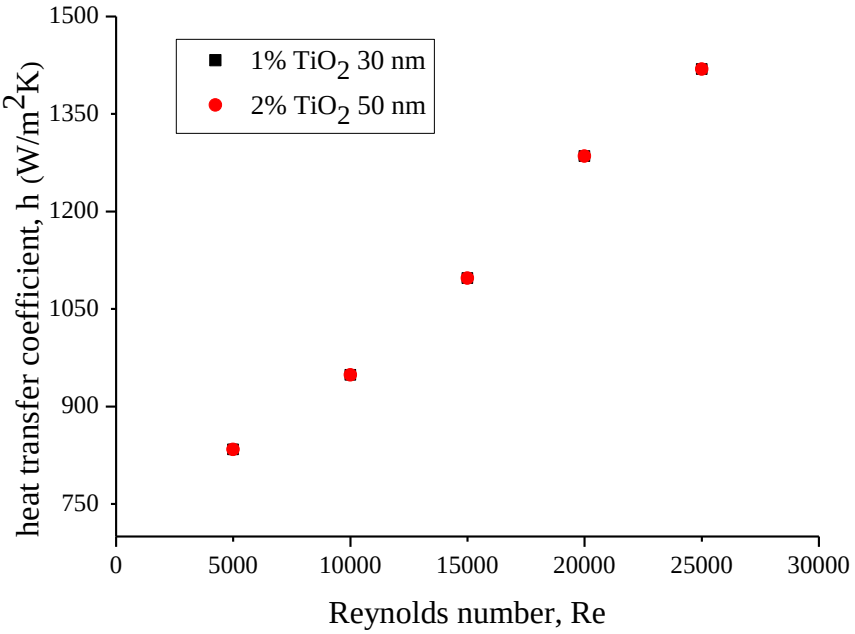

Figure 6.18: Heat transfer coefficient variation with nanoparticale diameter.

Chapter 7

Conclusions and Future Scope

7.1 Conclusions

1. With the use of twisted tape, the maximum increase in heat transfer coefficient is observed for twist ratio of 3.2 and the increase is in the range of 1.34 - 1.36 times as compared to the heat transfer coefficient of plain tube. The friction factor for twist ratio of 3.2 is 2.1 times that of simple tube.

2. The increase in heat transfer coefficient for 0.05% TiO_2 concentration is 4-6%. The friction factor of the nanofluid used in the experiment is nearly same as that of water since the concentration of nanoparticle used for the experiments is very less

3. For 0.05% TiO_2-water nanofluid with twisted tape insert of twist ratio 3.2, the heat transfer coefficient increase is up to 1.45 times that obtained when water is used in plain tube. Friction factor increase is found to be 2.1 to 2.2 times

4. The results obtained using ANSYS Fluent 14.5 is comparable to the experimental results. Also, for the nanofluid flow, the two phase model approach gives more accurate results than single phase approach. Results from ANSYS Fluent 14.5 shows that the maximum increase in heat transfer coefficient is 6%, 10.9%, 17.4% and 23.4% for TiO_2-water nanofluid with TiO_2 concentrations of 0.05%, 1%, 2% and 3%, respectively.

5. The increase in heat transfer coefficient is in the range of 9-11%, 20-27% and 21-30% for TiO_2-water, Al_2O_3-water and CuO-water nanofluid, respectively.

6. Variation of heat transfer coefficient with nanoparticle size is studied using CFD simulations by taking different diameters (30 nm and 50 nm) of TiO_2 nanoparticles. There is no difference in the heat transfer coefficient values for both the diameters considered at low volumetric concentrations (0.05%).

7.2 Future Scope

1. The heat transfer coefficient is found to be increasing by using nanofluid as working fluid with twisted tape inserts. But still the composition of the nanofluid after it passes through the tube with twisted tape inserts is unknown.
2. In the present study, in CFD simulations, the properties of water or nanofluid used is assumed to be constant. But the properties do change with change in temperature. Hence, further accurate results can be obtained by simulations if the properties are considered to vary with temperature. This can be done in CFD using User Defined Function (UDF) option.

References

Ahmed, H.E., Ahmed, M.I. & Yusoff, M.Z., 2015. Heat transfer enhancement in a triangular duct using compound nanofluids and turbulators. *Applied Thermal Engineering*, 91, pp.191–201. Available at: http://dx.doi.org/10.1016/j.applthermaleng.2015.07.061.

Akbari, M., Galanis, N. & Behzadmehr, A., 2011. Comparative analysis of single and two-phase models for CFD studies of nanofluid heat transfer. *International Journal of Thermal Sciences*, 50(8), pp.1343–1354.

Azmi, W.H. et al., 2014. Turbulent forced convection heat transfer of nanofluids with twisted tape insert in a plain tube. *Energy Procedia*, 52, pp.296–307. Available at: http://dx.doi.org/10.1016/j.egypro.2014.07.081.

Davarnejad, R., Barati, S. & Kooshki, M., 2013. CFD simulation of the effect of particle size on the nanofluids convective heat transfer in the developed region in a circular tube. *SpringerPlus*, 2(1), p.192.

Davarnejad, R. & Jamshidzadeh, M., 2015. Engineering Science and Technology , an International Journal Short communication CFD modeling of heat transfer performance of MgO-water nano fl uid under turbulent fl ow. , 18, pp.536–542.

Delavari, V. & Hashemabadi, S.H., 2014. CFD simulation of heat transfer enhancement of Al_2O_3/water and Al_2O_3/ethylene glycol nanofluids in a car radiator. *Applied Thermal Engineering*, 73(1), pp.380–390.

Demir, H. et al., 2011. Numerical investigation on the single phase forced convection heat transfer characteristics of TiO_2 nanofluids in a double-tube counter flow heat exchanger. *International Communications in Heat and Mass Transfer*, 38(2), pp.218–228.

Duangthongsuk, W. & Wongwises, S., 2009. Heat transfer enhancement and pressure drop characteristics of TiO_2-water nanofluid in a double-tube counter flow heat exchanger. *International Journal of Heat and Mass Transfer*, 52(7-8), pp.2059–2067.

Elsayed, A. et al., 2015. Numerical investigation of turbulent flow heat transfer and pressure drop of Al_2O_3 /water nanofluid in helically coiled tubes. *International Journal of Low-Carbon Technologies*, 10(3), pp.275–282.

Ghozatloo, A., Rashidi, A. & Shariaty-Niassar, M., 2014. Convective heat transfer enhancement of graphene nanofluids in shell and tube heat exchanger. *Experimental Thermal and Fluid Science*, 53, pp.136–141. Available at: http://dx.doi.org/10.1016/j.expthermflusci.2013.11.018.

Haghshenas Fard, M., Esfahany, M.N. & Talaie, M.R., 2010. Numerical study of convective heat transfer of nanofluids in a circular tube two-phase model versus single-phase model. *International Communications in Heat and Mass Transfer*, 37(1), pp.91–97. Available at: http://dx.doi.org/10.1016/j.icheatmasstransfer.2009.08.003.

Hameed, M. et al., 2015. Engineering Science and Technology , an International Journal Study of magnetic and heat transfer on the peristaltic transport of a fractional second

grade fl uid in a vertical tube. , 18, pp.496–502.

Hejazian, M. & Moraveji, M.K., 2013. A Comparative Analysis of Single and Two-Phase Models of Turbulent Convective Heat Transfer in a Tube for TiO 2 Nanofluid with CFD. *Numerical Heat Transfer, Part A: Applications*, 63(10), pp.795–806. Available at: http://www.tandfonline.com/doi/abs/10.1080/10407782.2013.756759.

Hemmat Esfe, M. et al., 2014. Thermophysical properties, heat transfer and pressure drop of COOH-functionalized multi walled carbon nanotubes/water nanofluids. *International Communications in Heat and Mass Transfer*, 58, pp.176–183. Available at: http://dx.doi.org/10.1016/j.icheatmasstransfer.2014.08.037.

Kalteh, M. et al., 2011. Eulerian-Eulerian two-phase numerical simulation of nanofluid laminar forced convection in a microchannel. *International Journal of Heat and Fluid Flow*, 32(1), pp.107–116.

Kamyar, A., Saidur, R. & Hasanuzzaman, M., 2012. Application of Computational Fluid Dynamics (CFD) for nanofluids. *International Journal of Heat and Mass Transfer*, 55(15-16), pp.4104–4115.

Keshavarz Moraveji, M. & Esmaeili, E., 2012. Comparison between single-phase and two-phases CFD modeling of laminar forced convection flow of nanofluids in a circular tube under constant heat flux. *International Communications in Heat and Mass Transfer*, 39(8), pp.1297–1302.

Kumar, p.c.m. Et al., 2012. Heat transfer enhancement in a helically coiled tube with Al_2O_3 /water nanofluid under laminar flow condition. *International journal of nanoscience*, 11(05), p.1250029.

Lelea, D. & Nisulescu, C., 2011. The micro-tube heat transfer and fl uid fl ow of water based Al 2 O 3 nano fl uid with viscous dissipation ☆. , 38, pp.704–710.

Madhesh, D., Parameshwaran, R. & Kalaiselvam, S., 2014. Experimental investigation on convective heat transfer and rheological characteristics of Cu-TiO2 hybrid nanofluids. *Experimental Thermal and Fluid Science*, 52, pp.104–115.

Mahdavi, M., Sharifpur, M. & Meyer, J.P., 2015. CFD modelling of heat transfer and pressure drops for nanofluids through vertical tubes in laminar flow by Lagrangian and Eulerian approaches. *International Journal of Heat and Mass Transfer*, 88, pp.803–813. Available at: http://dx.doi.org/10.1016/j.ijheatmasstransfer.2015.04.112.

Moraveji, M.K. & Ardehali, R.M., 2013. CFD modeling (comparing single and two-phase approaches) on thermal performance of Al_2O_3/water nanofluid in mini-channel heat sink. *International Communications in Heat and Mass Transfer*, 44, pp.157–164. Available at: http://dx.doi.org/10.1016/j.icheatmasstransfer.2013.02.012.

Namburu, P.K. et al., 2009. Numerical study of turbulent flow and heat transfer characteristics of nanofluids considering variable properties. *International Journal of Thermal Sciences*, 48(2), pp.290–302.

Naphon, P. & Suchana, T., 2011. Heat transfer enhancement and pressure drop of the horizontal concentric tube with twisted wires brush inserts. *International Communications in Heat and Mass Transfer*, 38(2), pp.236–241.

Navaei, A.S. et al., 2015. Heat transfer enhancement of turbulent nanofluid flow over various types of internally corrugated channels. *Powder Technology*, 286, pp.332–341. Available at: http://dx.doi.org/10.1016/j.powtec.2015.06.009.

Sekhar, Y.R. et al., 2013. Heat transfer enhancement with Al2O3 nanofluids and twisted tapes in a pipe for solar thermal applications. *Procedia Engineering*, 64, pp.1474–1484. Available at: http://dx.doi.org/10.1016/j.proeng.2013.09.229.

Sun, B., Lei, W. & Yang, D., 2015. Flow and convective heat transfer characteristics of Fe2O3-water nanofluids inside copper tubes. *International Communications in Heat and Mass Transfer*, 64, pp.21–28.

Timofeeva, E. V et al., 2011. Nanofluids for heat transfer: an engineering approach. *Nanoscale research letters*, 6(1), p.182.

Vajjha, R.S., Das, D.K. & Kulkarni, D.P., 2010. Development of new correlations for convective heat transfer and friction factor in turbulent regime for nanofluids. *International Journal of Heat and Mass Transfer*, 53(21-22), pp.4607–4618.

Zhao, N. et al., 2016. Numerical investigations of laminar heat transfer and flow performance of Al_2O_3-water nanofluids in a flat tube. *International Journal of Heat and Mass Transfer*, 92, pp.268–282.

Appendix

Table A1: Experimental data for double tube heat exchanger with twisted tape insert of $y_o/W = 6$.

Mass flow rates (lpm)	T_{h1}	T_{h2}	T_{c1}	T_{c2}	Pressure drop (cm of mercury)
1	62.3	45.4	27.4	30.5	0.7
2	62.5	50.1	27.5	31.5	2.4
3	62	52.6	27.5	32.5	5.3
4	62.2	54.4	25.7	31.9	9.3
5	62.1	56.1	26.8	34.5	14.8

Table A2: Experimental data for double tube heat exchanger with twisted tape insert of $y_o/W = 4$.

Mass flow rates (lpm)	T_{h1}	T_{h2}	T_{c1}	T_{c2}	Pressure drop (cm of mercury)
1	62.3	45.4	27.4	31.1	0.9
2	62.5	51.2	27.5	32.8	2.9
3	62	53.8	27.5	34.2	6.4
4	62.2	55.7	25.7	33.7	10.5
5	62.1	56.2	26.8	35.4	16

Table A3: Experimental data for double tube heat exchanger with twisted tape insert of $y_o/W = 3.2$.

Mass flow rates (lpm)	T_{h1}	T_{h2}	T_{c1}	T_{c2}	Pressure drop (cm of mercury)
1	62.3	45.4	27.4	31.1	1.2
2	62.5	51.2	27.5	32.8	3.9
3	62	53.8	27.5	34.2	8.6
4	62.2	55.7	25.7	33.7	14
5	62.1	56.2	26.8	35.4	20

Table A4: Experimental data for double tube heat exchanger with working fluid as TiO_2-water nanofluid of TiO_2 concentration 0.05%

Mass flow rates (lpm)	T_{h1}	T_{h2}	T_{c1}	T_{c2}	Pressure drop (cm of mercury)
1	62.5	49.7	25.3	30	0.6
2	62	51.5	26.2	31	1.9
3	62.2	54.1	25.3	31.7	4.1
4	62.2	56.5	25.1	32.8	6.5
5	62.7	57.4	25.7	34.1	9.6

Table A5: Experimental data for double tube heat exchanger with working fluid as TiO_2-water nanofluid of TiO_2 concentration 0.026%

Mass flow rates (lpm)	T_{h1}	T_{h2}	T_{c1}	T_{c2}	Pressure drop (cm of mercury)
1	61.9	50	26	30.5	0.6
2	62.3	52	26.1	30.9	1.9
3	62.2	54	25.8	31.6	4.1
4	61.8	56.6	25.8	33.3	6.5
5	62.1	57.3	25.9	34.2	9.6

Table A6: Experimental data for double tube heat exchanger with working fluid as TiO_2-water nanofluid of TiO_2 concentration 0.05% and twisted tape insert with twist ratio of 6.

Mass flow rates (lpm)	T_{h1}	T_{h2}	T_{c1}	T_{c2}	Pressure drop (cm of mercury)
1	61.5	45.3	27.3	30.9	0.7
2	62.1	49.8	27.1	32	2.4
3	61.2	52.3	27.2	33	5.3
4	61	54	27.3	34	9.3
5	61.3	55.1	27.5	35.1	14.8

Table A7: Experimental data for double tube heat exchanger with working fluid as TiO_2-water nanofluid of TiO_2 concentration 0.05% and twisted tape insert with twist ratio of 4.

Mass flow rates (lpm)	T_{h1}	T_{h2}	T_{c1}	T_{c2}	Pressure drop (cm of mercury)
1	62	44.2	26.8	30.6	0.9
2	61.8	48.5	27	31.7	2.9
3	62.2	50.8	27.2	32.4	6.4
4	62.3	53.2	27.3	33.5	10.5
5	62	55	27.2	35.3	16

Table A7: Experimental data for double tube heat exchanger with working fluid as TiO_2-water nanofluid of TiO_2 concentration 0.05% and twisted tape insert with twist ratio of 3.2.

Mass flow rates (lpm)	T_{h1}	T_{h2}	T_{c1}	T_{c2}	Pressure drop (cm of mercury)
1	62.5	43.1	27.3	31.4	1.2
2	62.4	49.2	27.2	32.8	3.9
3	62	51.4	27.5	33.8	8.6
4	62.3	52.2	27.4	33.9	14
5	62	54.4	27	35.7	20

Table A7: Experimental data for double tube heat exchanger with working fluid as TiO_2-water nanofluid of TiO_2 concentration 0.026% and twisted tape insert with twist ratio of 6.

Mass flow rates (lpm)	T_{h1}	T_{h2}	T_{c1}	T_{c2}	Pressure drop (cm of mercury)
1	62.3	45.1	27.4	30.5	0.7
2	62.5	49.9	27.5	31.6	2.4
3	62.3	52.5	27.5	32.7	5.3
4	62.1	54.2	25.7	32	9.3
5	62.3	56.3	26.8	34.7	14.8

Table A7: Experimental data for double tube heat exchanger with working fluid as TiO_2-water nanofluid of TiO_2 concentration 0.026% and twisted tape insert with twist ratio of 4.

Mass flow rates (lpm)	T_{h1}	T_{h2}	T_{c1}	T_{c2}	Pressure drop (cm of mercury)
1	61	45.2	27.1	30.9	0.9
2	61.3	47.5	27	31	2.9
3	61.2	51	27.3	32.6	6.4
4	61.5	53.5	27.4	33.6	10.5
5	61	55.1	27.1	35.4	16

Table A7: Experimental data for double tube heat exchanger with working fluid as TiO_2-water nanofluid of TiO_2 concentration 0.026% and twisted tape insert with twist ratio of 3.2

Mass flow rates (lpm)	T_{h1}	T_{h2}	T_{c1}	T_{c2}	Pressure drop (cm of mercury)
1	62.5	44.1	27.3	31.4	1.2
2	62.1	49.2	27.2	32.8	3.9
3	62.2	51.5	27.5	33.7	8.6
4	62	52.2	27.3	33.9	14
5	62.3	54.4	27.5	35.7	20

.

ME_Thesis

ORIGINALITY REPORT

16%	2%	16%	3%
SIMILARITY INDEX	INTERNET SOURCES	PUBLICATIONS	STUDENT PAPERS

PRIMARY SOURCES

1	Heat Transfer Enhancement of Heat Exchangers, 1999. Publication	1%
2	Duangthongsuk, W.. "Heat transfer enhancement and pressure drop characteristics of TiO"2-water nanofluid in a double-tube counter flow heat exchanger", International Journal of Heat and Mass Transfer, 200903 Publication	1%
3	Ganesan, P., I. Behroyan, S. He, S. Sivasankaran, and Shanti C. Sandaran. "Turbulent forced convection of Cu–water nanofluid in a heated tube: Improvement of the two-phase model", Numerical Heat Transfer Part A Applications, 2015. Publication	1%
4	Submitted to Universiti Tenaga Nasional Student Paper	1%
5	Chougule, Sandesh S., and S.K. Sahu. "Heat transfer and friction characteristics of Al2O3/water and CNT/water nanofluids in	1%